Critical Reviews in Biochemistry and Molecular Biology, 28(4):323–367 (1993)

Photochemical Reactions in Organized and Semiorganized Media

Katsuhiko Takagi and Yasuhiko Sawaki

Department of Applied Chemistry, School of Engineering, Nagoya University, Chikusa-ku, Nagoya 464-01, Japan

Referee: Prof. Michel Chanon, Universite de Proit, D'Economie et des Science D'Aix-Marseille III, Faculte des Sci. et Tech. de Saint-Jerome, Ave. Escadrille Normandie, Niemen-bolte 561-13397, Marseille, France

ABSTRACT: The article describes organic photochemical reactions in heterogeneous fields. The first part of the article includes an introduction of miscellaneous electrostatic fields adsorbing photoactive species and the second part summarizes the types of photochemical reactions in their fields. Photochemical reactions carried out in various heterogeneous fields, inorganic as well as organic, were classified by their reaction type, that is, unimolecular reactions, bimolecular reactions, energy transfer reactions, and electron transfer reactions.

KEY WORDS: photochemical reactions, organized media, electrostatic interfaces, micelles, vesicles, polyelectrolytes, silica, clay, zeolite, miscellaneous types of reactions, energy transfer, electron transfer.

Common abbreviations in the present article are listed as follows: AEC, anion exchange capacity; AOT, aerozol OT; AQDS, sodium anthraquinonedisulfonate; BHDB, benzylhexadecyldimethylammonium bromide; cmc, critical micelle concentration; CTAB, cetyltrimethylammonium bromide; CTAC, cetyltrimethylammonium chloride; CEC, cation exchange capacity; CT, charge transfer; DAP, dodecylammonium propionate; DBA, 1,3-dibutylalloxazine; DCP, sodium dicetylphosphate; DDDAC, didodecydimethylammonium chloride; DPC, 1-dodecylpyridinium chloride; DPL, dipalmitoyllecithin; DQ^{2+}, α,α-dipyridium ion; EDTA, ethylenediamine tetraacetic acid; EPE, poly(ethylene oxide-propylene oxide ethylene oxide); FMN, flavin mononucleotide; FMNH, dihydroflavin mononucleotide; KDC, potassium dodecanoate; syn-HH, syn-head-to-head dimer; anti-HH, anti-head-to-head dimer; syn-HT, syn-head-to-tail dimer; In, indole detergent; LB, Langmuir-Blodgett; MB, methylene blue; MV^{2+}, methyl viologen; MW, molecular weight; N_A, aggregation number; P, pyrene; PA, pyrene-3-carboxaldehyde; P18C6, poly(vinylbenzo-18-crown); PSSNa, sodium poly(styrenesulfonate); RV^{2+}, alkyl viologen; SDS, sodium dodecyl sulfate; Tc, phase-transition temperature; TEtOA, triethanolamine; ZnTPPS, zinc(II) tetrasodiumtetra(*p*-sulfonatophenyl)porphyrin; ZnTPP, zinc(II) tetraphenylporphyrin; ZnTPyP, zinc(II) tetra(*N*-methylpyridinium)porphyrin; ZnTPSPy, zinc(II) tetra(*N*-sulfonatopropylpyridinium)porphyrin.

I. INTRODUCTION

It is most urgent and valuable for chemists to develop a highly selective methodology for preparation of what is wanted. Photosynthesis by green plants or enzymatically catalytic reactions by common living organisms are precious examples for chemists. These marvelous bioreactions take place in organized microheterogeneous fields. Thus, photosynthesis is carried out in cell membranes of green plants where the photochemical reaction center is composed of light-absorbing species (photosensitizer) and electron transfer mediators, and the combined redox system is disposed elaborately as a completely organized system. The mutual disposition of each component is essential for the photochemical system; otherwise, no net chemical reaction is observed.

When photoreactive compounds are irradiated under geometrically confined circumstances, they are compelled to undergo a directed reaction course. An increasing number of investigations are concentrating, to mimic bioreactions, on studies of highly selective reactions in microheterogeneous systems. However, the use of microheterogeneous systems for photochemical reactions is still in its

1040-9238/93/$.50

infancy. This is mostly because of the high complexity of such systems. Extensive exploration of photochemistry in these microheterogeneous systems is expected to open new areas of photofunctional science as well as synthetic photochemistry.

The present article is a survey of photochemical reactions carried out in microheterogeneous reaction fields. These heterogeneous fields include micelles, reversed (or inverse) micelles, vesicles, Langmuir-Blodgett (LB) films, and also inorganic solid surfaces such as silica, clay minerals, and zeolite cavities, as shown in Figure 1. Photocatalytic reactions using semiconductor metal oxides are omitted because of restriction of space.

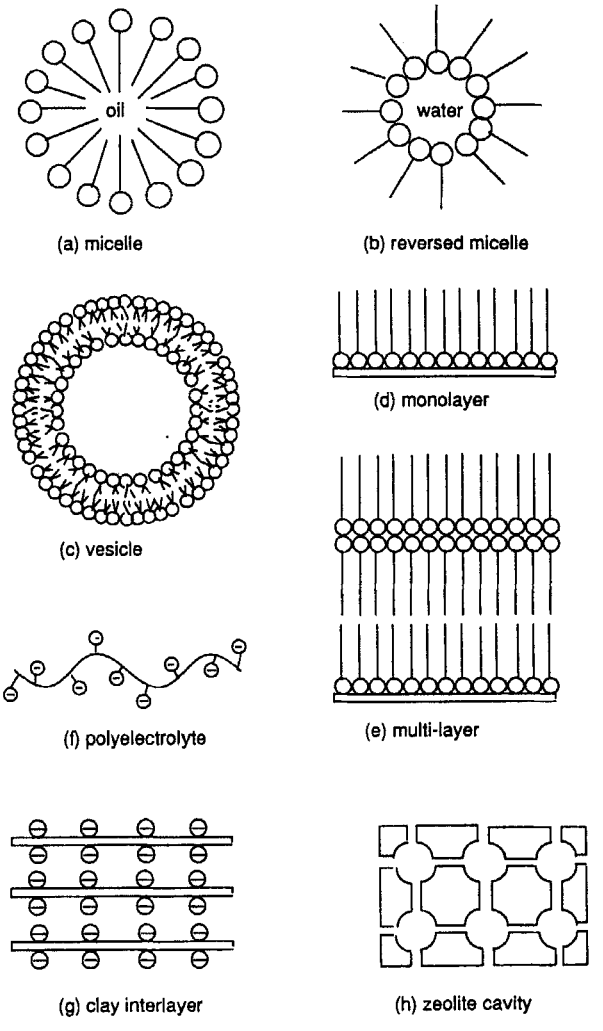

FIGURE 1. Schematic pictures of typical ionic interfaces.

II. ELECTROSTATIC INTERFACES FOR PHOTOCHEMICAL REACTION FIELDS

A. Surfactant Assemblies

1. Micelles and Reversed Micelles

Aqueous micelle solutions are easily accessible and excellent reaction media. Hence, numerous examples have been reported on organized photochemical reactions in conventional aqueous micelles.[1] In general, surfactants are amphiphilic molecules with both hydrophobic and hydrophilic groups. When these amphiphilic molecules are dispersed in water, the hydrophilic part is easily solvated, whereas the hydrophobic part resists the solvation by water. The hydrophobic interaction between the hydrocarbon chains and the repulsion from solvent water are responsible for the aggregation of surfactant molecules.

The surfactant molecules form molecular aggregates, that is, micelles, in water at concentrations higher than their critical micelle concentrations (cmc). Sodium dodecylsulfate (SDS; cmc, 8.1 m*M*) is a typical anionic surfactant, and cetyltrimethyl-ammonium bromide (CTAB; cmc, 0.92 m*M*) is a cationic surfactant.

A simplified model for ionic micelles pictured by Hartley[2] is useful for visualization (Figure 2). According to the model, micelles are roughly spherical and contain 50 to 200 surfactant molecules. Their radii are close to the lengths of the hydrocarbon chain of

$CH_3(CH_2)_{11}OSO_3Na$ SDS $CH_3(CH_2)_{15}N(CH_3)^+_3Br^-$ CTAB

surfactants, that is, 10 to 30 Å. The micelle has a hydrocarbon core and a polar surface; it resembles an oil drop with a polar coat. The head groups of ionic micelles and associated counterions are found in the compact Stern layer. Some of the counterions are bound on the surface, but most are located in the electrical double layer (up to several hundred angstroms), as shown in Figure 2. Organic guest molecules are solubilized in the core or at the interface of the micelles, depending on their hydrophobicity or hydrophilicity. The volume of the aggregate is estimated at 3.99×10^4 Å,^{3} half of which is occupied with the inner hydrophobic

core and the rest with the Stern interface layer. Resulting solubilities of typical organic compounds in ionic micelles are summarized in Table 1. Solubilities of organic substrates into micellar interiors are shown to be profoundly dependent on their molecular structures. Benzene and α-methylstyrene, for example, can be solubilized up to an approximately equal amount with the surfactants; that is, several tens of substrate molecules can be accommodated in one SDS micelle. For other substrates tested, one to several molecules can be dissolved as guest substrates in a micelle.

Some amphipathic materials form molecular aggregates in hydrophobic solvents, for example, hexane, benzene, and chloroform. These are called a reversed (or inverse) micelle in comparison with the usual micelles in water. Typical surfactants for reversed micelles are sodium *bis*(2-ethylhexyl)sulfosuccinate (AOT), dodecylammonium propionate (DAP), and didodecyldimethylammonium chloride (DDDAC). They form linear aggregations at lower concentrations, but produce, especially in the presence of water droplets, spherical reversed micelles at higher concentrations.[3]

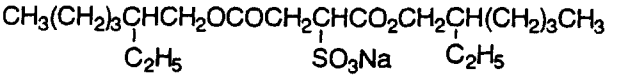

AOT

DAP DDDAC

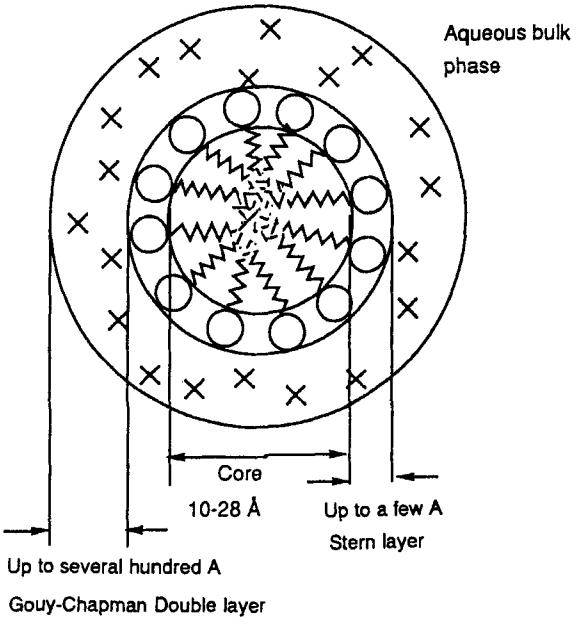

FIGURE 2. A simplified two-dimensional picture of a spherical ionic micelle. O~~: Surfactant molecules; ×: counterion. (From Fendler, J. H., *Membrane Mimetic Chemistry*, Wiley-Interscience, New York, 1982, 6. With permission.)

Aqueous micelles provide an excellent organized reaction field but, at the same time, are accompanied with a weak point in that the solubilities of guest molecules are not always sufficient and product isolations are tedious. Therefore, most photochemical studies relating to micelles are inclined to use physicochemical processes, for example, photosensitized electron transfers. Micelle surfaces are effective for a charge separation between an electron donor and an acceptor as will be discussed later. On the other hand, a large enough amount of guest molecules should be solubilized to make use of micelles for preparative scale experiments. For such a purpose, a few methods have been attempted: (1) modification of guest molecules by substituting with a long alkyl chain that is dissolvable in host surfactant aggregates; (2) utilization of a microemulsion system, in which guest molecules are codissolved with hydrophobic organic solvents in micelles; (3) formation of a 1:1 complex of ionic guest molecules with an opposite charge.

Modification of guest molecules by method 1 is sometimes accepted and significantly improves

TABLE 1
Solubility of Some Organic Compounds in Ionic Micelles

Guest molecules	Solubility (m*M*/100 m*M* surfactant)[a]	
	CTAB	SDS
Benzene	100	—[b]
α-Methylstyrene	67	—[b]
Stilbene	5.3	—[b]
4-Methyoxystilbene	5.0	4.5
4,4′-Dimethoxystilbene	0.2	—[b]
1,1-Diphenylethylene	4.0	4.1
Phenylvinylether	4.5	4.8
9,10-Dicyanoanthracene	0.018	—[b]
1-Cyanonaphthalene	0.007	—[b]
1,8-Dinitronaphthalene	1.0	—[b]

[a] Excess amounts of guest molecules were added to a 100 m*M*-aqueous micellar solution and the dissolved substrates were determined after sonication for 60 min at 20°C.
[b] Not measured.

Usami, K., Takagi, K., and Sawaki, Y., unpublished results.

their solubilities. It should be remembered, however, that the presence of a long alkyl chain often makes the product separation difficult. The utilization of microemulsion systems (method 2) is not always useful because the stability of emulsion and solubility of substrates are lower. Method 3 is the most convenient way to solubilize guest ionic molecules into a micelle or a reversed micelle. Thus, *N,N*-dimethyllaurylammonium hydroxide forms a salt with various guest carboxylic acids, which then forms a micelle in water. For the workup after photolysis, a simple extraction with organic solvents, for example, diethyl ether from HCl-acidified photolysate solution, is enough for a preferential separation of reacted carboxylic acids. Reversed micelles in hydrophobic organic solvents are more convenient for product isolation. A 1:1 salt of acidified AOT and guest tertiary amines makes a reversed micelle in organic solvents such as dichloromethane or benzene. Workup operation is also easy; addition of aqueous NaOH to the photolysate, followed by extraction with CH_2Cl_2, gives starting amines and their photoproducts no contamination from the surfactant.

It is intriguing to know how guest molecules, when incorporated in micelles, are conformationally organized in the structured micelle environment. To monitor properties of micellar aggregates, probe molecules, which exhibit fluorescence or absorption spectra characteristic to solubilization sites are sometimes used. A typical example of a fluorescence probe is pyrene. Kalyanasundaram and Thomas[4] have found a profound polarity effect on the ratio of the first (373 nm) and the third (385 nm) peak intensities of the structured fluorescence spectrum of pyrene, that is, I_{373}/I_{385}; for example, solubilization sites for pyrene molecules in SDS micelles were deduced to be significantly polar and close to those of ethanol. The intensity ratios (I_{373}/I_{385}) are linearly correlated with absorption maxima of charge transfer (CT) bands between stilbenes and methyl viologen (MV^{2+}) in aqueous anionic micelles.[5]

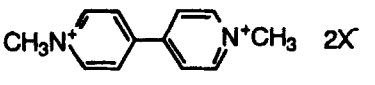

MV^{2+}

Ionically charged surfactants such as CTAB and SDS adsorb oppositely charged substrates electrostatically. For example, cationic micelles bind carboxylate and phenolate anions, and anionic micelles bind quaternary ammonium ions, including protonated amines. Because these ionic substrates are hydrophilic, it is not clear whether or not they are absorbed on the micelle surface. A fluorescence probe to observe the solubilization sites can be applied on the basis of quenching efficiency by guest molecules as quenchers.[6–8] Thus, the fluorescence of zinc(II) tetra(*p*-sulfonate)phenylporphyrin (ZnTPPS) is quenched efficiently by 1,2-dibromocinnamate in the presence of CTAB micelles.[9] Figure 3 shows that an anionic SDS micelle has no effect on the quenching between anionic ZnTPPS and 1,2-dibromocinnamates. On the other hand, the quenching in the presence of a cationic CTAB micelle is efficient because of efficient electrostatic adsorption of oppositely charged ZnTPPS and 1,2-dibromocinnamate ions. A discontinuous

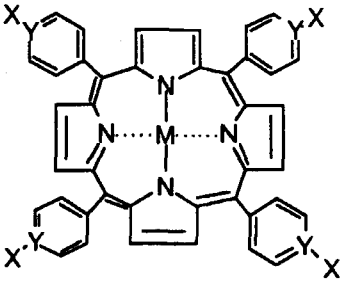

ZnTPPS: M = Zn; X = SO_3Na; Y = C

ZnTPP: M = Zn; X = H; Y = C

ZnTPyP: M = Zn; X = CH_3; Y = N^+

ZnTPSPy: M = Zn; X = $CH_2CH_2SO_3^-$; Y = N^+

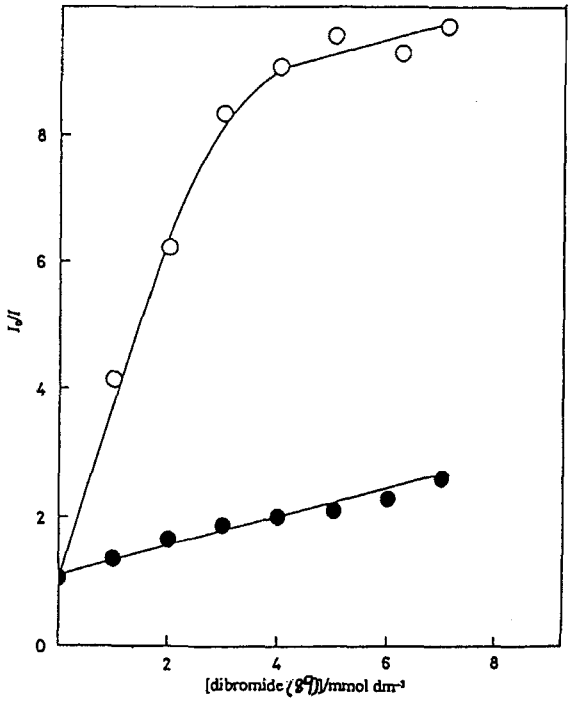

FIGURE 3. Quenching of 9-methylanthracene fluorescence by the dibromide anion in CTAB (○) and SDS (●) micelles. Conditions: 9-methylanthracene, 0.1 m*M*; surfactant, 4 m*M*; irradiation, 290 ± 2 nm; detection of its fluorescence, 390 nm. (From Takagi, K., Miyake, N., Nakamura, E., Usami, H., and Sawaki, Y., *J. Chem. Soc. Faraday Trans. 1*, 84, 3475, 1988. With permission.)

point can be seen in a relationship between the fluorescence intensity and the dibromide concentrations in CTAB micelle solutions. Because the discontinuous point appears at the equimolar concentration, that is [CTAB] = [cinnamate], it is apparent that one surfactant molecule adsorbs just one cinnamate ion and the excess amount of cinnamate ions are dissolved in the bulk water solution. Hence, a discontinuous point determines the maximum solubilization ability of the micelle. Usually, ionic micelles are capable of accommodating oppositely charged organic ions equal to their aggregation numbers (N_A). The structure of the rigid and immobile SDS micelles at 77 K in an ethyleneglycol-water mixture has been characterized by luminescence-quenching studies.[10] These rigid micelles provide a unique electrostatic field that fixes guest molecules in a known geometry.

Amphiphilic ionic pairs can be easily prepared by mixing SDS with alkyl ammonium halides or mixing CTAB with sodium alkyl carboxylates, followed by extraction with

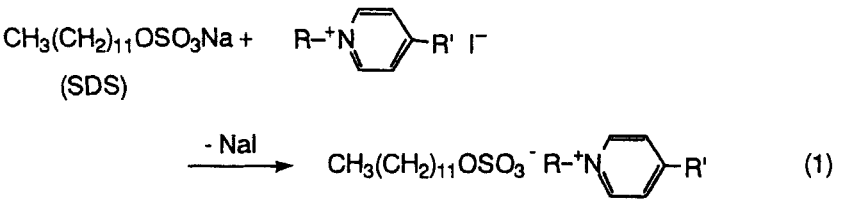

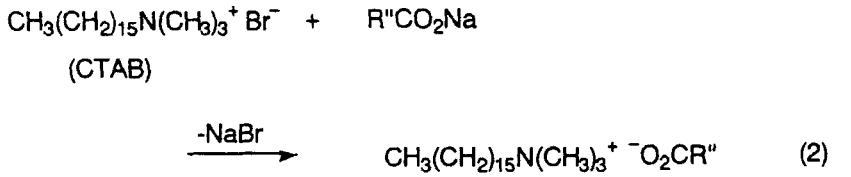

hydrophobic solvents such as CH_2Cl_2 and benzene (Equations 1 and 2). Thus obtained amphiphilic ion pairs form micelles and sometimes vesicles that are characteristic to self-associating reaction fields. Sometimes ionic substrates, for example, carboxylates or protonated amines with long alkyl chains, are able to form micelles or premicelle aggregates. Aggregation numbers of amphiphilic ion pairs and surfactant substrates have been reported to be measured by means of nuclear magnetic resonance (NMR) spectrophotometry[11a,b,12] or by using fluorescence probes[13,14a,b] as well as directly by a light-scattering method.[14b] According to the methods of Equations 1 and 2, propionic acid and laurylamine form 1:1 aggregates with N_A of 3 to 7 in cyclohexane, whereas SDS and *N*-methylstilbazolium iodide form micelles with N_A of 63, which is close to those in aqueous SDS micelles.

2. Vesicles

Vesicles are aggregates much larger than micelles, having a spherical or ellipsoidal closed bilayer structure, as shown in Figure 4.[15] Aggregates from phospholipids are termed liposomes. As shown in Figure 4, polar head groups of the lipids are exposed to the aqueous phase on both sides of the bilayer, and hence, the hydrocarbon chains align themselves in the inner core forming the bilayer. When guest molecules are included in such a molecular aggregate, it is interesting to know how they are organized and how their molecular conformation affects photochemical reactivities.

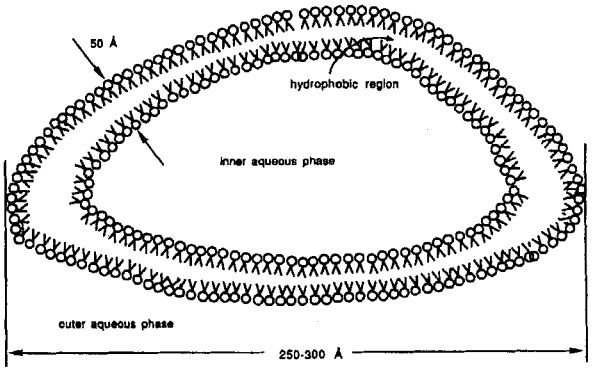

FIGURE 4. Schematic representation of a liposome bilayer.

Lipid vesicles and liposomes are known to have phase-transition temperatures (Tc) on which the alignment of surfactant molecules in the bilayers is changed. As explained in the previous case of micelle systems, the relative intensities of vibronic bands in pyrene fluorescence, I_{373}/I_{385}, can be applied to study the polarity of the solubilization sites. That is, pyrene was found to be solubilized in a polar region near the polar head groups below Tc, whereas it migrates into the nonpolar hydrophobic core region above Tc.[16a,b] At least two different solubilization sites probably exist in the vesicles. Solubilization sites of guest molecules also are dependent on the properties of guest molecules. Dipalmitoyllecithin (DPL) vesicle, for example, is reported to accommodate 4,4′-disubstituted *trans*-stilbenes **(1–3)** on its polar interface or in an organized bilayer region, depending on the

chain length of the alkyl substituents; that is, they are solubilized in the polar interface region in cases of shorter chain length but in the bilayer core in cases of longer chains.[17] Other evidence for the solubilization sites also was presented by measuring the rates of bromination of substituted stilbenes in DPL vesicles, where the bromination satisfied a two-component, first-order rate equation.[18] Triplet decay rates of 4-nitro-4′-methoxystilbene are sensitive to the polarity, viscosity, and pH of their microenvironments. Their triplet decay was divided into two components, that is, slower and faster decays, which are interchangeable with each other depending on the reaction temperature related to Tc.[19]

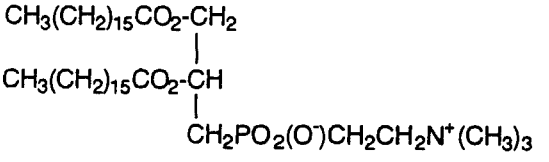

DPL

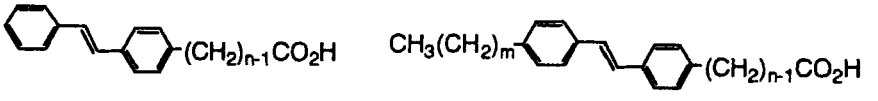

1 (n = 4-16) 2 (m,n = 2-8)

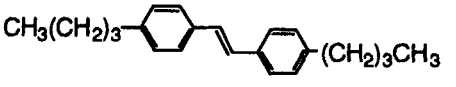

3

No example is available for the utilization of vesicle systems for preparative-scale photochemical reactions. Vesicle aggregates, however, provide an excellent system for photochemical charge separation on both aqueous compartments insulated by bilayers. Interestingly, photochemical electron transfers across vesicles are closely related to natural photosynthesis taking place in thylakoid membranes. As will be described later, the most important aspect is the realization of a net charge separation on some organized interfaces after a photochemical electron transfer between photosensitizer and electron acceptor. A large number of articles have been published concerning electron transfers in such systems.

3. Monolayered and Multilayered Membranes

When surface-active agents are spread on water, they form a monolayer film, directing their hydrophobic alkyl chains toward the air phase on the surface of the water. Successive deposition of monolayers on appropriate supports affords a multilayer assembly. Monolayers or multilayers transferred from the air-water interface to glass slides are called Langmuir-Blodgett (LB) films, and they have opened fruitful fields for controllable photochemical molecular devices.[20a,b]

The most advantageous point of monolayer or multilayer assemblies is based on the artificially controllable arrangement of surfactant aggregates. Therefore, the layered assemblies are suitable for investigating photochemical energy or electron-transfer processes between organized donors and acceptors, indicating the importance of intermolecular alignments. Although some stereoselective photodimerizations have been noted,[21a,b] the LB films are not suitable for preparative scale photoreac-

tions; this is because the LB films are not always stable and the scaleup is difficult.

B. Polyelectrolytes

Polyelectrolytes interact intimately with oppositely charged surfactants.[22a–25] For example, micelle clusters were formed on dispersion in water when sodium poly(styrenesulfonate) (PSSNa) formed a complex with CTAB. This means that cationic substrates may be adsorbed on polyelectrolyte aggregates. In fact, thousands of stilbazolium ions can be effectively adsorbed in one strand of PSSNa, which has been found to have micelle-like clusters.

Polyelectrolyte PA-18K_2 forms a compact coil at lower pH and an extended rod or coil at higher pH. The polyelectrolyte can bind cationic or anionic pyrene derivatives on its micelle-like compact coil. Thus, PA-18K_2 with a molecular weight (MW) of 10,000 forms a polymer micelle composed of about 25 monomer units as confirmed by using a pyrene fluorescence probe.[26] Similarly, poly(acrylic acid) exists as a coil at lower pH and

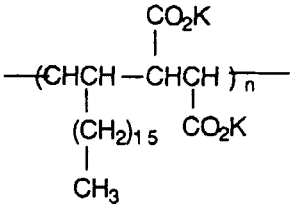

PA–18K_2

as an expanded form at higher pH, which was supported by lack of visible pyrene excimer fluorescence at high pH regions.[27] Addition of CTAB to the poly(methacrylic acid) solution yields micelle-like aggregates in which 100-CTAB molecules are accommodated. Quenching studies using a pyrene excimer probe were successful in determining the N_A values of polyelectrolyte complexes in combination with 1-dodecylpyridinium chloride (DPC) as a quencher.[28] Poly(styrenesulfonate) also forms a micelle-like cluster with stilbazolium ions, the N_A of which is estimated at about 100.[29]

The structure of hydrophilic aggregates of poly(ethylene oxide-propylene oxide-ethylene oxide)(EPE) block copolymer was investigated by using three kinds of fluorescence probes,[30] an indole detergent (In), pyrene (P), and pyrene-3-carboxaldehyde (PA). Fluorescence maxima of In and PA and the intensity ratio of the I_{373}/I_{385} of pyrene fluorescence show that hydrophobicity of EPE is increased with increasing pressure and with decreasing temperature. As a fluorescent probe for polyelectrolytes, dansyl group[31,32] and diphenylanthracene[33] also are reported.

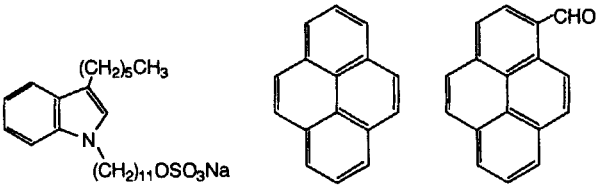

In P PA

Polysoap, poly(vinylbenzo-18-crown-6) (P18C6) adsorbs pyrenylbutylammonium ion[34] and other species.[35] The pyrenyl groups are inserted between adjacent crown ether ligands, with the $-NMe_3^+$ group protruding into the aqueous phase.

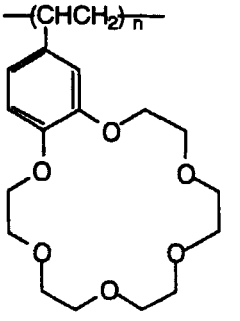

P18C6

C. Inorganic Electrostatic Fields

The solid surface of inorganic materials, for example, silica, clay minerals, and zeolites, possesses anionic or cationic sites absorbing charged guest molecules electrostatically. These inorganic minerals are photochemically inert, which is in contrast to the known photochemical activities of metal oxide semiconductors. In the present section, the properties of inorganic materials as electrostatic reactions are outlined briefly.

1. Silica Surfaces

Silica colloids consist of negatively charged spherical particles with a diameter of 50 to 500 Å. The surface is covered by an electric double layer that is made up by SiO^- and OH^- and usually is neutralized by sodium ions. The sodium ions are easily exchangeable with organic cations.[36] In water, nearly complete substitution with organic cations often results in precipitation of substituted colloids, which sometimes become soluble in organic solvents.

It is interesting to note that nonexponential decay curves were observed for the fluorescences of azobenzene, triphenylmethane dyes, and thioindigo adsorbed on alumina or silica.[37] The nonexponential decays were discussed in terms of different aggregation sites on polarizing surfaces and of interference between directly emitted and scattered fluorescence radiation. When the silica surface is porous, the size of the cavity controls the approach of substrates, affecting photochemical reaction course. The term "porous" means "sponge-like" or "microscopic hole."[38] The surface area of porous silica usually reaches 1000 m^2/g as determined from N_2 gas adsorption. Cavities with a diameter >20 Å are effective as an adsorption site and the silanol groups are responsible for the magnetic interaction with guest molecules.

2. Clay Interlayers

Clays have layered structures and are readily suspended in aqueous solutions.[39a,b] Thus, montmorillonites are composed of units made up of two silica tetrahedral sheets and one alumina octahedral sheet, as illustrated in Figure 5. Their intersheet layer includes exchangeable metal ions (e.g., sodium ions), neutralizing net negative charges yielded by partial substitution of Si^{4+} by Al^{3+} at the tetrahedral sites. This is the reason why montmorillonites tend to adsorb cationic species and are readily suspended in water. On the contrary, some clays, for example, hydrotalcite, include exchangeable negative ions, leading to the effective adsorption of negatively charged guest molecules. The properties of typical clays are summarized in Table 2.

The numbers of exchangeable ions of clay minerals determine the amounts of organic guest ions that can be intercalated between the clay layers. For example, montmorillonite clay is capable of adsorbing guest cations according to a magnitude of cation exchange capacity (CEC), which is expressed as milliequivalents of the anionic sites per unit gram of the clay. Likewise, hydrotalcite accommodates guest anions according to a magnitude of anion exchange capacity (AEC) expressed as milliequivalents of the cationic sites per unit gram of the clay. Efficiencies of intercalations are dependent on the types of clays and guest molecules.[40-42] Adsorption on clays is accomplished by adding equimolar ionic substrates to aqueous colloidal clay solutions, sonicating with an ultrasound mixer, thus sometimes resulting in precipitations. In most cases, intercalated clay colloids can be homogeneously dispersed in hydrophobic solvents such as benzene, chloroform, and dichloromethane. A long-chain alkyl ammonium ion, for example, cetyltrimethylammonium ion (CTAC), forms its double layer on laponite clay surface.[43] Nonionic materials also may be intercalated in clay interlayers.[41,42]

A fluorescence probe can be used to study adsorption behaviors on clay interlayers. The emission maximum of an $Ru(bpy)_3^{2+}$ ion on clay minerals shifted toward a longer wavelength linearly, depending on the negative charge of the lattice and on the average particle size.[44] This was interpreted in terms of the distribution of the ion molecules over the external surface (i.e., edge sites) and the interlayer surface (i.e., planar sites).[44] DeSchryver et al.[45] reported on a fluorescent probe of pyrenes with ammonium groups, the conformation of which changed, depending on the degree of intercalation and the presence of coadsorbents. Hydrophobic pyrene itself was shown to be adsorbed as a monolayer on dry smectite clay and laponite.[46]

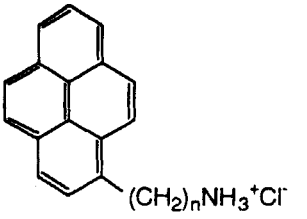

PnN (n = 1-3)

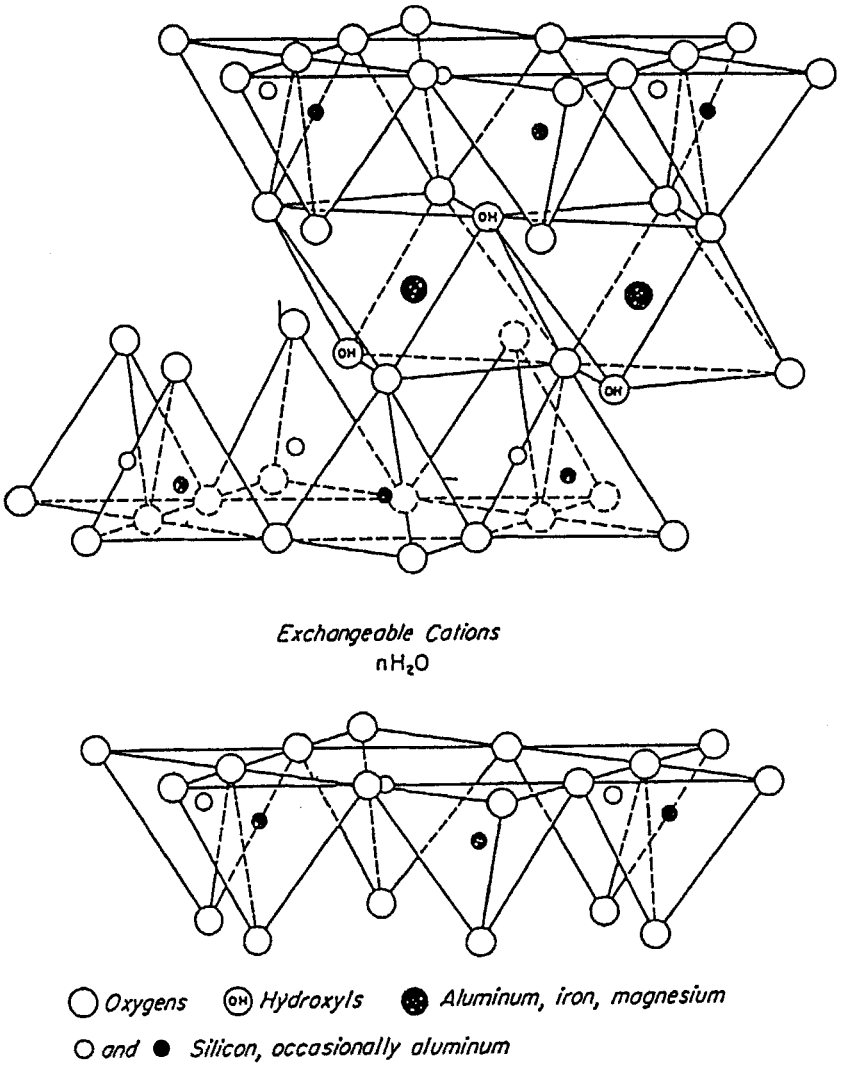

FIGURE 5. A structure of montmorillonite.

TABLE 2
Properties of Typical Clay Minerals

Clay	Layer structure[a] [SiO_4/AlO_4]	Exchangeable ion	Ion exchange capacity (mEq/100 g)
Montmorillonite	~2/1	Na^+, Ca^{2+}	60–80
Saponite	~2/1	Na^+, Ca^{2+}	60–80
Vermiculite	~2/1	Mg^{2+}, Ca^{2+}	100–150
Kaoline	~1/1[b]		2~10
Hydrotalcite	[MgO_2]Octahedral	OH^-, CO_3^-	~400

[a] Molar ratio of SiO_4/AlO_4 if not specified.
[b] The ratio of SiO_4/AlO_4 or SiO_4/MgO_2.

Desorption of pyrene was accomplished simply by adding water to give microcrystals of pyrene. Micropolarity of environments for pyrene molecules was increased by eliminating water on the basis of changing the ratio of pyrene fluorescence intensities, I_{373}/I_{383}, from 0.9 to 1.80.

The conformation of a pyrene-labeled poly(acrylic acid) adsorbed at the water-alumina solid interface was made clear by using a fluorescence probe of pyrene excimer, indicating coiling structure of the strand.[47] The adsorbed polymer was shown to be extended at high pH but coiled at lower pH region.

Application of clay minerals to organized photochemical reactions has revealed an interesting aspect forced by spatial confinement in clay interlayers. The following features are shown: (1) not only cationic or anionic substrates, but also nonionic polar substrates, can be efficiently accommodated in the interlayers; (2) long alkyl-chain guest molecules such as CTAB can be arranged in a uniform manner, similar to those of LB membranes; (3) intercalation of some surfactants, for example, CTAB, makes the clay particles dissolvable in typical hydrophobic solvents such as benzene, dichloromethane, or carbon tetrachloride; and (4) clay colloids adsorbing organic guests form essentially transparent films by a simple casting or filtration *in vacuo*.

3. Zeolite Cavities

Zeolites[48a–c] are porous inorganic materials constituted from tetrahedral metal oxides, AlO_4 and SiO_4, forcing guest molecules to be subject to three-dimensional steric confinement. A zeolite cavity includes, as in the case of clay, alkaline metal cations exchangeable with some guest ions. Zeolites are classified into hydrophilic and hydrophobic types, called zeolite X or Y and silicalite, respectively (Table 3). The structure of X- or Y-type zeolite consists of (as shown in Figure 6) a cavity of 13 Å in diameter linked by a path of 8 to 10 Å in diameter that may accommodate hydrophilic guest molecules. Silicalite possesses an inner cavity of 5 to 6 Å in diameter and adsorbs hydrophobic guest molecules.

Organic molecules included in zeolite cavities are known to exhibit characteristic emissive properties. Several aromatic ketones, such as acetophenone, benzophenone, and β-phenylpropiophenone, in zeolite show readily detectable phosphorescence at room temperature with a lifetime of 0.18 to 0.30 ms.[49] Thus, the lifetime of excited triplet β-phenylpropiophenone at room temperature is enhanced by about five orders of magnitude on inclusion into the channels of silicalite with hydrophobic cavity.[50a] This is attributed to the restricted mobility in the cavity. On the basis of nonexponential phosphorescence decay of the ketone triplet, silicalite has been proved to have at least two distinct inclusion sites. Pyrene fluorescence intensity ratio (I_{375}/I_{385}) indicates a very polar medium for pyrene in zeolites X (0.45) and Y (0.74). Quenching of excited purene by oxygen gas is quite efficient, indicating a concentration of O_2 in the zeolite, similar to that in the gas phase.[50b]

There is an intrinsic difference between zeolite cavities and clay interlayers; that is, the capacity of zeolite cavities is not enough to accom-

TABLE 3
Representative Molecular Sieve Zeolites

Zeolite	Type	[AlO_4/SiO_4]	Channel (Å)	Diameter of cavity (Å)
A	Faujasite	1/1	4	11
X		1/2.2 ~ 1/3	8	13
Y		1/2.6	8	13
L	Chabazite	1/1	3.7	
ZSM-5	Pentasil Zeolite	1/31	—	—
Silicalite		~1/20	5.4	—
Mordenite		~1/5	3 × 6	7

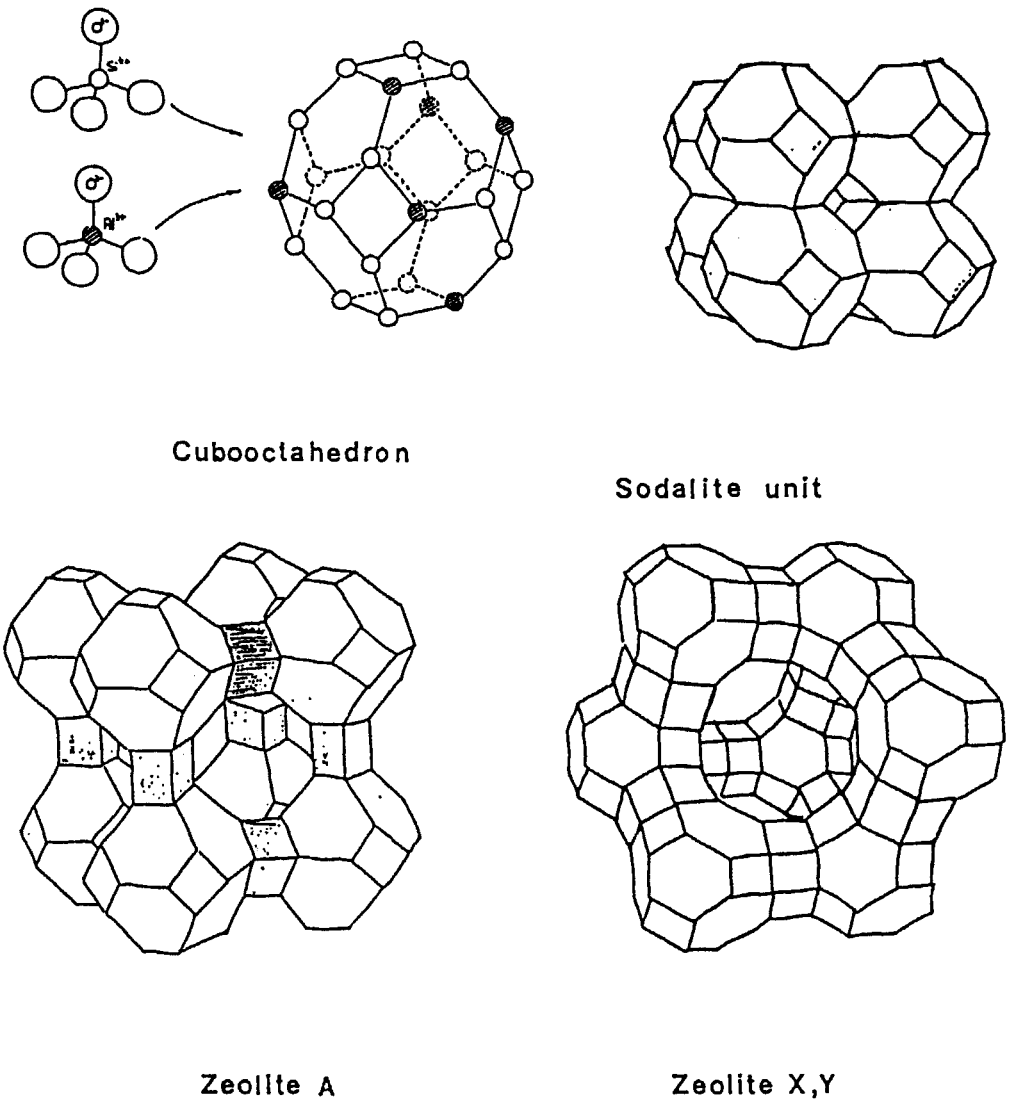

FIGURE 6. Schematic representation of the structural features of zeolites A, X, and Y and their constituted units. (From Van Hooff, J. H. C., *Chemistry and Chemical Engineering of Catalytic Process, NATO Advanced Studies Institute Series E, No. E39,* Prias, R. and Schuit, G. C. A., Eds., Sijthoff & Noordhoff Publishers, The Netherlands, 1980, 161. With permission.)

modate more than three molecules of guests or reagents, which implies no occurrence of intermolecular reactions or photochemical electron transfers. Unique unimolecular reactions, however, can be expected in such a spatially confined reaction field. These aspects are different from the case of clay interlayers in which intermolecular reactions are easily accessible because of the intercalation of many guest molecules.

III. PHOTOCHEMICAL REACTIONS ON ELECTROSTATIC FIELDS

A. Unimolecular Reactions

1. Isomerizations

Photoisomerization between *cis*- and *trans*-olefins is one of the most significant photochemical reactions. The process is closely related to an

induction of excitation of the visual nerve of animals via the stereoselective isomerization of the 11-*cis* retinal moiety into the all-*trans* form of rhodopsin. *Cis-trans*-photoisomerizations of olefins are quite useful for the preparation of *cis*-olefins, and the reaction media sometimes affect the isomerization because of their polarity, viscosity, or solubility. Hence, microheterogeneous fields such as micelles, vesicles, and monolayer or bilayer membranes would be expected to function as organized media controlling photoreaction pathways.

Substituted stilbenes (**1–3**) with different chains were subjected to photochemical *cis-trans*-isomerization in SDS micelle, DPL, and sodium dicetylphosphate (DCP) vesicles.[17] The substituted stilbenes were solubilized in different sites in these heterogeneous fields. Suddaby et al.[17] concluded that the inner phase of SDS micelles is similar to homogeneous solutions and the micelles have no effect on the photochemical isomerization. In contrast, DPL or DCP vesicles provide an organized environment in which the structural change of adsorbed stilbenes is restricted and exhibits a discontinuous point at their phase-transition temperature, Tc.

4-Hydroxy-1-cetylstilbazolium betaine **4**, an amphiphilic merocyanine dye, is photoisomerized reversibly with comparable efficiency either in a benzyldimethylammonium chloride (BDAC) reversed micelle or in methanol.[51]

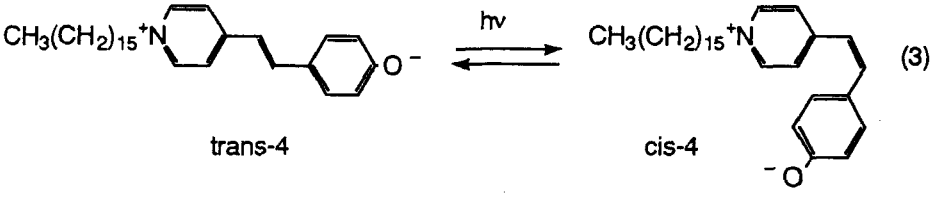

trans-4 cis-4 (3)

Photoisomerizations affording a mixture of *cis*- and *trans*-olefins were much faster than the photocyclodimerization when cinnamic acid,[52] 1,2-dinaphthylethylene,[53] and benzothiazovinylinidenetriazenes[54] were irradiated in micelle solutions. An interesting and selective formation of *trans*-stilbene was attained by applying silicalite. Thus, irradiation of *cis*-stilbene was done in the presence of silicalite using 3,4-dimethylbenzophenone as a sensitizer. *Trans*-stilbene (*trans*-5) once formed is intercalated selectively in a silicate cavity of 6 Å diameter, resulting in the irreversible transformation into pure *trans*-isomer.[55]

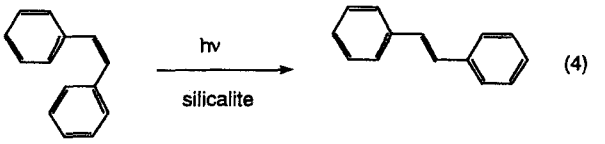

cis-5 trans-5 (4)

As will be described later, stilbazolium cation[56a–c] and cinnamate anion[57] can be efficiently intercalated in montmorillonite and hydrotalcite clays, respectively. Interestingly, the major photochemical reactions of the clay-intercalated olefins were not the *cis-trans*-isomerizations but their cyclodimerizations, implying that the restricted reaction fields govern the photoreactivity.

Adsorption of retinal (**6**) on silica gel shifts its absorption maximum by 50 nm to a longer wavelength. UV irradiation of adsorbed retinal gave rise to 11-*cis*-retinal at the photostationary state along with a mixture of several isomers (Table 4). A preferential isomerization to 11-*cis*-isomer was explained by the stereoelectronic effect of olefin rather than the polar effect of the silica gel surface.[58]

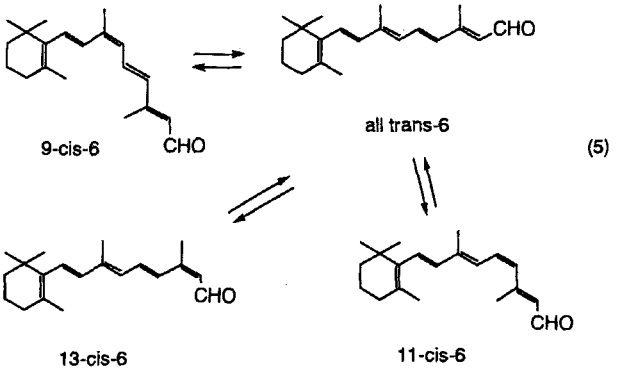

9-cis-6 all trans-6 (5)

13-cis-6 11-cis-6

TABLE 4
Product Distribution on Irradiation of All *trans*-Retinal (All-*trans*-6)

	Quantum yield		Photostationary state			
Medium	**All *trans*→9-*cis***	**All *trans*→13-*cis***	**All *trans***	**9-*cis***	**11-*cis***	**13-*cis***
Hexane	—	—	70	5	0	24
3-Methylpentane	0.015	—	—	—	—	—
Ethanol	—	—	53	7	20	25
Methanol	0.0006	0.0018	—	—	—	—
SiO_2/hexane	0.018	0.11	29	22	36	12

Alumina selectively adsorbs *cis*-thioindigo, but not the corresponding *trans*-isomer. Because of the stereospecific adsorption, a one-way photoisomerization takes place from *trans* to *cis*.[59] *Cis*-thioindigo adsorbed on alumina was shown to be photochemically inert.

2. The Norrish Type I and II Reactions

Photolysis of carbonyl compounds results in homolytic α-fissions and/or γ-hydrogen abstractions. The former is called Norrish type I, and the latter Norrish type II reaction (Equation 6).

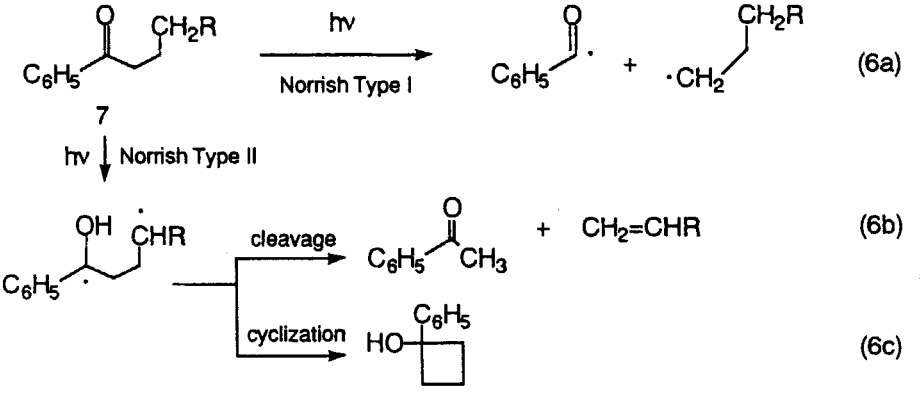

It appears that the Norrish type II reaction is dependent on the reaction media on the basis of its stereochemical requirements for the intramolecular hydrogen abstraction via a six-membered transition state. Hence, the Norrish type II reaction via the cyclic transition state would be unfavorable under the conditions of spatially restricted environments. The quantum efficiencies for the photochemical reaction of butyrophenone (7, R=H) are summarized in Table 5. The data in Table 5 suggest that butyrophenone, when incorporated in LB membrane, is constrained and unfavorable for the the cyclic transition state.[60a,b] Almost equal efficiencies in either the micelle or the usual solvents show that there is no significant difference in viscosity between them. This is in accordance with an observation that the micelle interior is disordered and not as viscous as *tert*-butanol.[61] When butyrophenone is incorporated in the LB membrane of arachidic acid, neither type I nor type II reaction takes place at all. In the LB membrane, butyrophenone is assumed to be organized as rigid molecular aggregates, and hence, the radical pairs, once they are formed, tend to recombine facilely, yielding the original ketone.

TABLE 5
The Quantum Yields for Photolysis of Butyrophenone (7, R=H)

Reaction media	$\Phi_{Type\ II}$
Tert-butanol	1.02 ± 0.03
SDS micelle	0.80 ± 0.02
CTAC micelle	0.72 ± 0.02
Benzene	0.27 ± 0.03
LB membrane	<0.001

The ratio of cyclization (Equation 6c) to β-fission (Equation 6b) in the Norrish type II reaction is dependent on the rigidity of the reaction media. In particular, the most striking effect was observed in the case of liquid crystal media. Thus, the ratios discontinuously increase with the increasing space rigidity of butyl stearate matrices in the order of isotropic, smectic, and solid phase by lowering the temperature.[62] The Norrish type II reaction is more rigorously inhibited by more restricted reaction fields consisting of inorganic zeolite; that is, silicalite-intercalated valerophenone (**7**, $R=CH_3$), on irradiation, is exclusively subject to β-elimination.[63] However, on intercalation in X-type zeolite with a larger space volume (i.e., 13 Å), the cyclization to cyclobutanol occurs and is comparable to β-elimination.[63] The increasing size of alkali metal ions from Li^+ to Cs^+ in the zeolite cavity also is shown to affect the ratio of cyclization to β-fission.[64a,b] Singlet and triplet excited state lifetimes depend on the identity and accessibility of the cation present within the supercage of X-type fauzasite zeolite (Li, Na, K, Rb, Cs, Tl). Thus, the phosphorescence-to-fluorescence intensity ratio for acenaphthene in zeolite X with Cs^+ is about 1000 higher than that with Li^+.[64c]

Photodecarbonylation of dibenzylketone (**8**) to yield bibenzyl and carbon monoxide is a typical Norrish type I reaction (Equation 7).[65,66] The photolysis of unsymmetrical dibenzyl ketone (**9**) in solutions gave two kinds of homo (A-A and B-B) and crossed bibenzyls (A-B) in

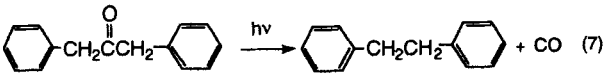

(7)

8

a ratio of 1:1:2. The ratio was significantly changed, however, by the presence of CTAB micelles. A statistical ratio (i.e., AA:AB:BB~ 1:2:1) was observed when the surfactant concentrations were much smaller than that of A(C=O)B (**9**). When the surfactant concentration was close to that of ketone or cmc, only the crossed dimer was produced. This is because the micelles act as a solvent cage that confines the resulting radical pair.

(8)

9

Turro et al.[67a,b] reported an interesting observation of enrichment of ^{13}C in **8** during the photodecarbonylation of ^{13}C-labeled **8** as indicated in Equation 9. The triplet radical pair (**10**) formed in CTAB micelles either dissociates into free radicals forming bibenzyl and carbon monoxide or undergoes intersystem crossing (isc) to yield a singlet radical pair (**11**), leading to the starting ketone ^{13}C-**8**. The enrichment of ^{13}C in the recovered ketone **8** is explained by the enhanced isc of triplet radical pair **10** containing ^{13}C atoms.

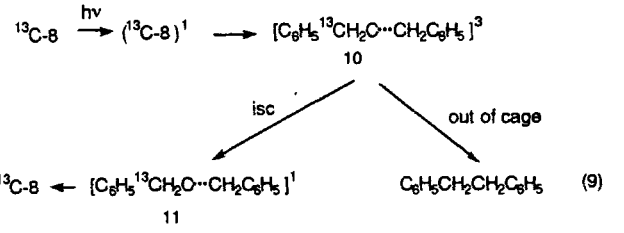

(9)

Addition of micelles is known to suppress the formation of radical-derived products in the Norrish type I reaction. Typical examples are the photolyses of dimethyldeoxybenzoin[68,69] and adamantylphenylketone.[70,71]

The photolysis of isomerically pure *d,l*- or *meso*-2,4-diphenylpentan-3-ones (**12**) adsorbed on X and Y zeolites resulted in the diastereoselective formation of 2,3-diphenylbutanes (**13**) in preference of *d,l*- over *meso*-isomers.[70] This is in sharp contrast to the reactions in homogeneous or micellar solutions having poor diastereoselectivity.[72]

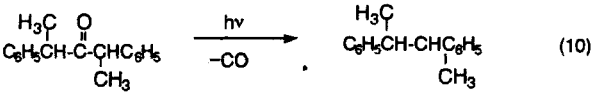

(10)

12 13

The Barton reaction of alkylnitrite (**14**) yields oxime (**16**) via O—NO homolysis to give **15**, intramolecular hydrogen abstraction, radical coupling followed by the isomerization to the oxime. This reaction was found to be inhibited by mi-

celles. There could be several explanations for this, including polarity of the media. No dramatic change, however, was observed in the photolysis in a variety of solvents, both polar and nonpolar.[73a] Because of its microviscosity, potassium dodecanoate (KDC) micelle retarded the Barton-type reaction involving the cyclic transition state to abstract hydrogen atom.[73b] Instead, the resulting alkoxy radical underwent disproportionation giving alcohol (**17**) and ketone (**18**).

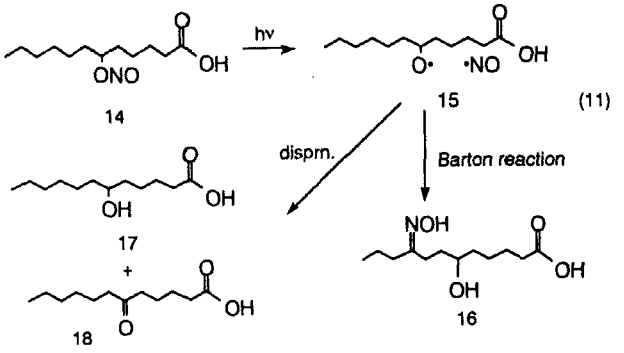

In contrast to micelle systems, silica gel adsorbs various hydrophobic organic compounds by means of hydrogen bonding, dispersion force, and/or electrostatic force. For example, carbonyl oxygen of ketone (**19**) is hydrogen bonded to the hydroxyl group of silica surface, which reduces the hydrogen abstraction of an excited carbonyl group by lowering its $n\pi^*$ nature; the Norrish type I reaction (Equation 12) becomes a major photoprocess.[74a] The lowest triplet state is reported to be π,π^* in nature in case of *p*-methoxyacetophenone embedded in Vycor glass.[74b] It is interesting to note that a zeolite cavity respects molecular sizes and controls product selectivity.

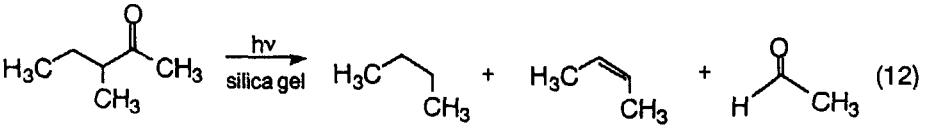

Thus, the photolysis of *o*-methyl bibenzyl ketone (**20**) in hydrophobic zeolite (ZSM, cavity diameter of 6 Å) gave only symmetrical dibenzyls (**21** and **23**), whereas the *p*-substituted benzyl radical yielded unsymmetrical dibenzyl (cf. **22**). Turro et al.[75a] explained that the *o*-substituted benzyl radical, but not the *p*-substituted benzyl radical, is too large to be accommodated in the cavity and therefore is diffused into the bulk. Unsubstituted and *p*-methyl-substituted benzyl radicals dimerize in the cavity, but the *o*-substituted benzyl radical dimerizes only in the bulk solution.

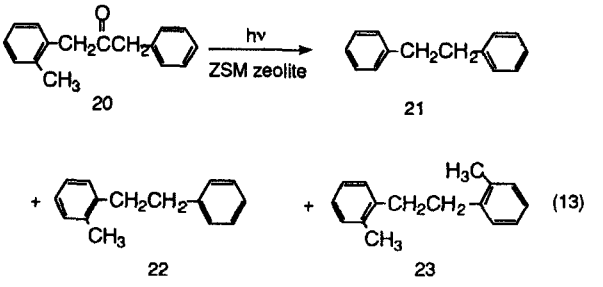

3. Rearrangements

A large number of radical-pair-type photo rearrangements are known to occur in homogeneous organic solvents. It is intriguing to see that molecular movements might be affected by organized media controlling rearranged products. Zeolites are crystalline aluminosilicates with cages and channel systems that can host a variety of organic transformations. This intracrystalline space is akin to a solvent and is describable in terms of solvatochromic indicators. For example, a faujasite zeolite includes a solvatochromic indicator in its cage as a zwitterionic form stabilized with Lewis acid (Na^+) and bases (oxygen of the framework).[75b]

Irradiation of **20** in X- or Y-type zeolites with larger cavities of a diameter about 13 Å was subject to a photo rearrangement to form **24** and **25**.[76a] In the restricted space of the cavity, radical pairs have longer lives, with time

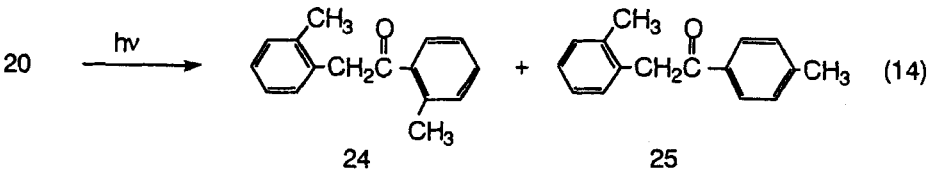

enough to rotate freely, leading to the observed rearrangement. Exchangeable cations in the zeolite cavity significantly affect product distribution.[76b,c] Going from Li^+ to Na^+ to K^+, rearranged products (e.g., **24** and **25**) are increased at the expense of the formation of diphenylethane (e.g., **22**). This is in correlation to the steady decrease of the amount of void space in a zeolite in the order from Li^+ to Na^+ to K^+. Product distribution from dibenzylketones was found to be dramatically dependent on the loading percentage of the starting ketone in zeolite. The amount of loaded ketones resulted in the increase of rearranged products and, at the same time, the decrease of diphenylethanes, which is explained by the rapid duffusion of the resulting radical pairs.[77] Photochemistry of zeolite-intercalated reactants is sensitive to simple coadsorbates such as water, benzene, cyclohexane, and hexane.[78a,b] Thus, the inclusion of organic molecules in the supercage of zeolite causes a significant congestion of void space and restricts the diffusional and rotational motion of radical pairs produced by the photolysis of **20.** As a result, the formation of **21–23** was suppressed, but the yields of **24** and **25** were increased; the addition of water caused a different result.[78] Preferential adsorption of water molecules in the cavity surface induced displacement of **20** to the external surface. Hence, the radical pair diffused freely and drastically decreased the formation of **24** and **25.**[76a,79]

The homolysis of cyclic ketone **(26)** in the zeolite cavity is reported to give ring-expanded ketone **(27),** as shown in Equation 15. This is contrasted to the results in solutions giving good yields of alkenols.[80,81] The molecular size of **26** with $n > 15$ is too large to be intercalated in the zeolite cavity. It is true, however, that the ring-expanded ketones **(27)** were formed in the cavity on irradiation in the presence of X-type zeolite. The typical photochemical reaction controlled by the zeolite cavity could be explained as radical pairs. Radical pairs formed by the photolysis of **26** can now enter the cavity and then cyclize at the *para* position of phenyl.[82]

deMayo et al.[83,84] noted that the photochemical Fries rearrangement of arylanilides **(28)** adsorbed on silica gel resulted in clearer reactions, although the yields of **30** and **31** were low compared with those in homogeneous solutions. The clear rearrangement on the silica surface was rationalized by assuming a difficult separation of radical-pair intermediates and their effective recombination.

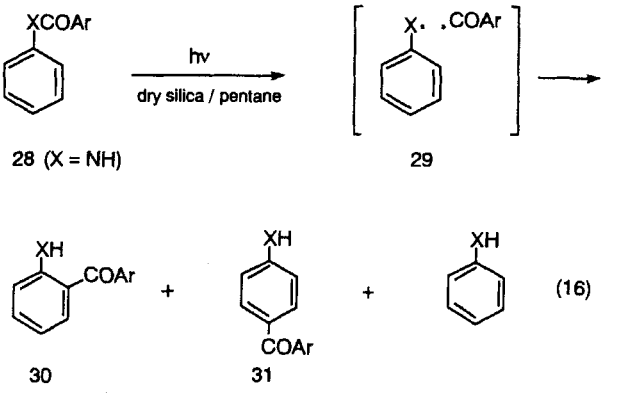

On UV irradiation, benzoin alkyl ethers and alkyl deoxybenzoins gave the rearranged benzophenones along with other photo products (Equation 17).[64]

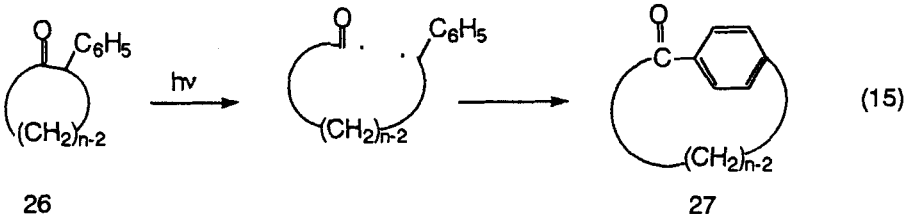

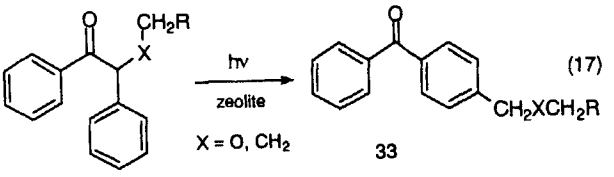

32 33

B. Bimolecular Reactions

1. Cyclodimerizations

Photochemical [2 + 2] cyclodimerizations are useful probes for understanding the alignment of olefin molecules, organized or not, in heterogeneous fields. Various types of organized media have been used for the cyclodimerizations. Thus, the photochemical cyclodimerization of 9-methylanthracenes[85] and 9-hydroxymethylanthracenes[86] is known to give head-to-head dimers, indicating their parallel orientation in CTAB and SDS micelles. In contrast, the cyclodimerization of acenaphthene was shown to be governed by the polarities of the solvents used. As shown in Figure 7, a linear relationship between log ([*syn*-dimer]/[*anti*-dimer]) and polarities also is true in the cases of SDS and dodecyltrimethylammonium iodide micelles.[87,88] This indicates that acenaphthene molecules are organized in electrostatic fields by micelles, in contrast to the case of anthracenes.

An interesting result was obtained for the photodimerization of surfactantized stilbazolium ions **34** (R=$C_{16}H_{34}$) dissolved in CTAB micelles. Stereochemistry of the resulting dimer was essentially *syn*-head-to-head (*syn*-HH), which is in sharp contrast to the dimer of *syn*-head-to-tail(*syn*-HT) in relatively highly concentrated solutions. The preferential formation of *syn*-HH dimer in CTAB micelles clearly reflects that the surfactant stilbazolium ions are aligned parallel on the CTAB micelle surface.[21a] A similar stereochemistry in

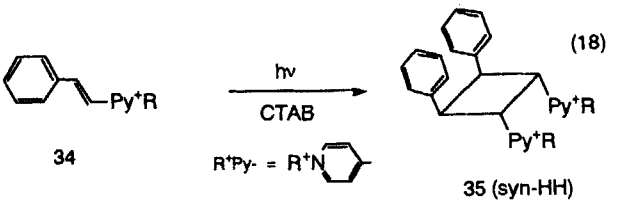

34 35 (syn-HH)

cyclodimers has been observed from olefins accommodated in bilayer membranes.[89,90]

Equimolar mixtures of protonated stilbazolium ions (**34,** R=H) with AOT anions form reversed micelles dissolvable in organic solvents, such as chloroform, carbon tetrachloride, and benzene. Aggregation of stilbazolium ions was evidenced by the fact that the micelle system exhibited a strong excimer fluorescence, whereas a homogeneous solution emitted only monomer fluorescence under similar concentrations. The ion pair in the reversed micelle yielded mainly the *syn*-HH dimer (**35**) along with minor formations of *syn*-HT and *anti*-HH dimers.[91] This reaction system is advantageous because of the simple and convenient procedure for product isolation; that is, the reactions mixture after irradiation was treated with concentrated HCl anthraquinone followed by the extraction with dichloromethane to give dimers. Reversed micelles contain water droplets of various sizes in their core. As shown in Table 6, a larger droplet lowered the stereoselectivity of the *syn*-HH dimer, implying a loosening of molecular packing in the reversed micelle.

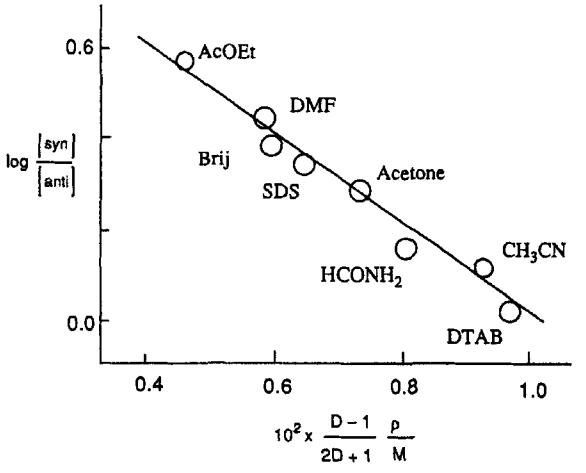

FIGURE 7. Dependence of log [syn]/[anti] on the solvent polarity, (D-1)/(2D+1) × n/*M* for the photochemical cyclodimerization of acenaphthene. (From Mayer, H., Schuster, F., and Sauer, J., *Tetrahedron Lett.*, 1289, 1986. With permission.)

TABLE 6
Effect of Water on Product Distribution from Photolysis of Stilbazolium Ion (34) in an AOT Reversed Micelle in Hexane

Initial concentration (*mM*)			Yield (%)			
[34] (R=H)	[AOT]	[H_2O]	*cis*-34	35	36	37
1.0	2.0	5	27	56	5	12
1.0	2.0	10	27	51	—	21
1.0	2.0	20	27	60	6	8
1.3	7.9	64	49	29	15	7
2.4	6.5	78	77	6	17	—

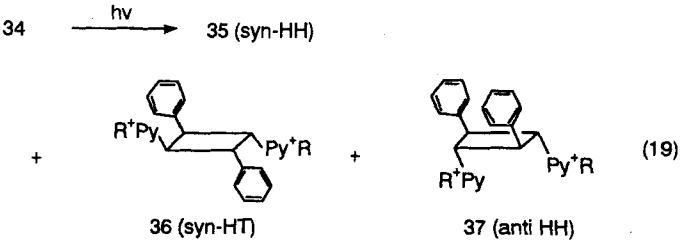

(19)

Cinnamic acids form ion pairs with laurylamine that are dissolvable in hydrophobic solvents as small aggregates consisting of several ion pairs. Irradiation of ion pair (**38**) resulted in the formation of *syn*- and *anti*-HH dimers (**39** and **40**) in a ratio of about 4:1.[52] The observed

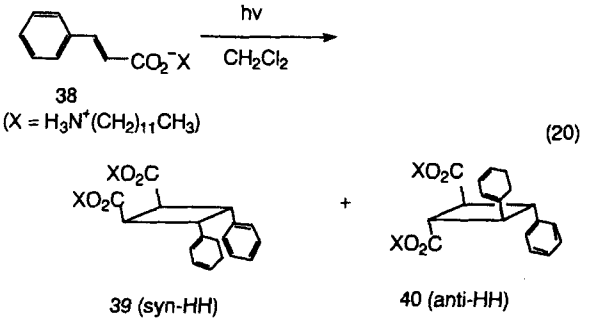

(20)

stereochemistry of the pair aggregates was different from that in solid state, where a *syn*-HT dimer was formed, reflecting the packing of the crystal structure. The quantum yield for the *syn*-HH dimer formation was significantly high (i.e., Φ 0.15), which is more than 20 times higher than that in the absence of laurylamine.

Another interesting point is a solvent effect for the stereoselectivity in the photodimerization of laurylammonium 2-indenecarboxylate (**41**).[92] Table 7 shows that the increasing polarity of solvents shifts a preferential dimer formation from *syn*-HH to *anti*-HH dimers. It is apparent that polar solvents may change molecular alignment in the reversed micelles in organic solvents.

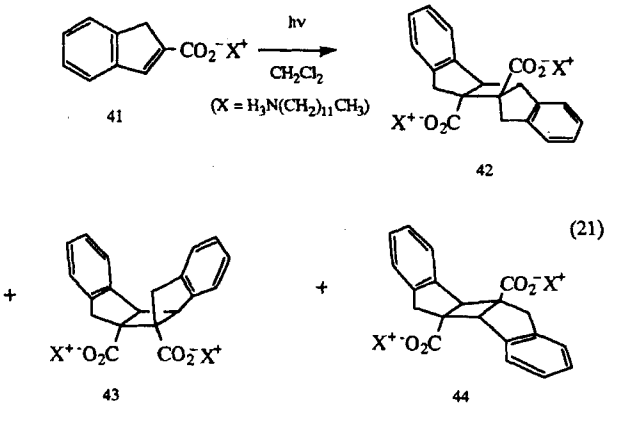

(21)

A contrasting result was obtained during the photolysis of 3-alkylcyclopentenone (**45**) in KDC micelles. Regioselectivities of HT- and HH-dimers were reversed by solvents, that is, benzene or KDC micelle.[93a,b] As listed in Table 8, the HH-

TABLE 7
Effect of Solvent on the Isomer Distributions from the Irradiation of Laurylammonium 2-Indene-Carboxylate (41)[a]

			Isomeric cyclodimer (%)		
X in 41	Solvent		42(*anti*-HH)	43(*syn*-HH)	44(*anti*-HT)
$H_3N(CH_2)_{11}Me$[b]	CH_2Cl_2	13	72	14	—
	C_6H_6	12	74	14	—
	C_6H_6[c]	10	74	16	—
	$CHCl_3$	19	54	28	—
	MeOH	85	—	11	4
	MeCN	88	—	12	—

[a] Conversion 30–55%.
[b] Irradiation time of 0.5 h.
[c] Dried by distillation over calcium hydride.

TABLE 8
Photochemical Cyclodimerization of 3-Alkylcyclopentenone (45)

Medium	46 (HT) (%)	47 (HH) (%)
Benzene	91	9
Methanol	50	50
KDC micelle	2	98

dimer was predominant in the micelle system. A preferential formation of HH-dimers in micelles also is noted in the photodimerization of isophorones[94] and coumarines.[95] The regiochemistry of the dimers is reasonably assumed to be a reflection of the mutual organized alignment of olefin molecules in micelles. Spherically structured aggregates, presented before as normal or reversed micelles (Figure 2), suggest similarly aligned molecules and seem to explain the observed regiochemistry of cyclodimers. Other examples also are shown here.[96,97]

Photodimerization of 2-methoxynaphthalenes (**48,** R=H) in SDS or CTAB micelles resulted in the exclusive formation of a demethylated product (**49**) through *cis*-dimer (Table 9).[96] This is in contrast to solution photochemistry, wherein only

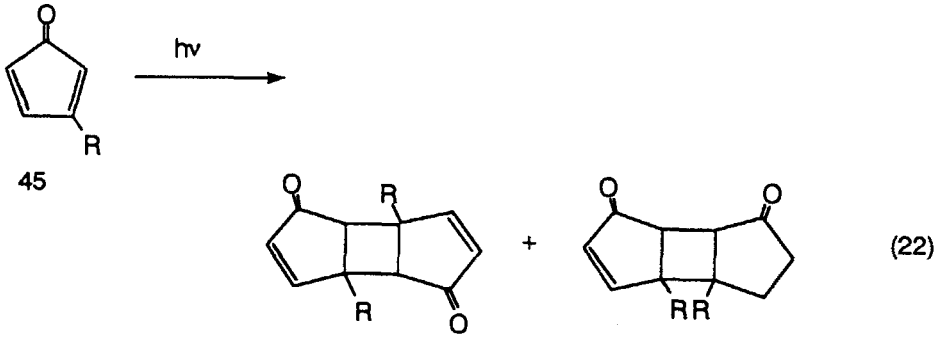

(22)

TABLE 9
Effect of Micelles on the Photocyclodimerization of 2-Methoxynaphthalenes (48)

Medium	49 *(cis)*		50 *(trans)*	
	R=H (%)	R=CH_3 (%)	R=H (%)	R=CH_3 (%)
Benzene	—	—	80	—
Cyclohexane	—	45	—	50
SDS micelle	60	45	—	—
CTAC micelle	71	61	—	—

the corresponding *trans*-dimer (**50**) is observed. These results are rationalized on the basis of the preorientation of **48** in micelles.

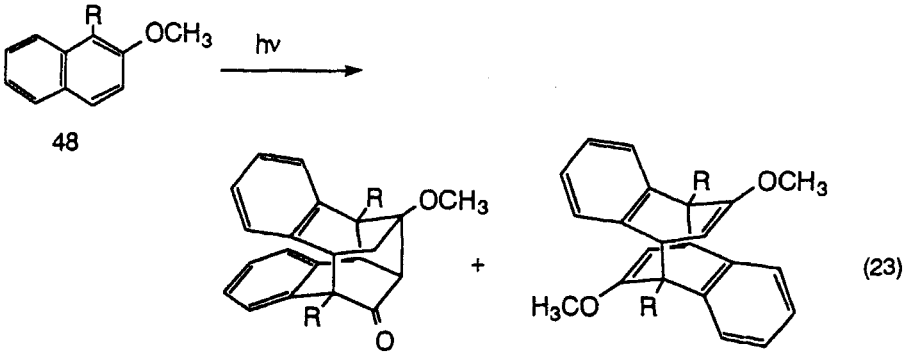

(23)

Similarly, irradiation of *N*-ω-carboxyalkyl-2-pyridone (**51**) in water gave rise to a random mixture of dimers, **52, 53, 54,** and **55** in yields of 48, 24, 14, and 14%, respectively. This implies that **51** dimerizes in a completely nonselective manner, approaching adjacent pyridones in homogeneous solutions. In contrast, the CTAB micelle is shown to regulate the orientation of the pyridones in its micelle interface on the basis of the exclusive formation of *cis*-isomers (**52:53:54:55** = 0:0:65:35).

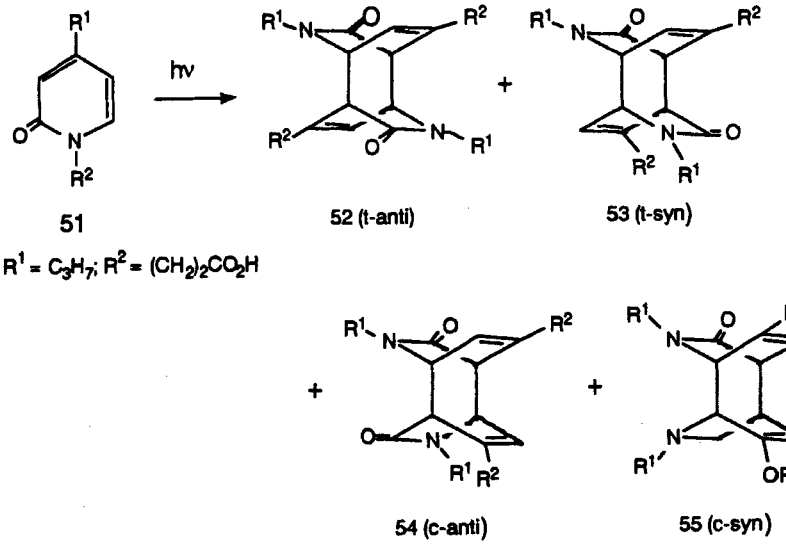

(24)

Photocyclodimerization occurred on the surface of the inorganic solid. That is, acenaphthene on silica surface (**56**) gave *cis*- and *trans*-cyclodimers.[98] It should be noted that a singlet excited acenaphthene formed an excimer with a

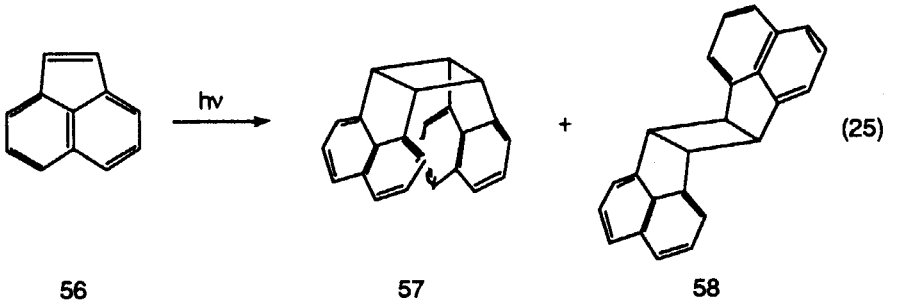

neighboring molecule, leading to the formation of a *cis*-dimer, whereas triplet excited **56** resulted in the formation of a *trans*-isomer via a stepwise radical pathway. The excited singlet (S_1) of **56,** because of its short lifetime (about 1×10^{-9} s), formed a complex only with the nearest olefin. On the other hand, the excited triplet acenaphthene may have diffused approximately 300 Å within its lifetime, 1×10^{-6} s. These factors are clearly reflected by the increasing *cis/trans* ratios with the increasing olefin molecules on SiO_2 surfaces, as shown in Figure 8. The rapid diffusion of some aromatic molecules on the surface has been measured using time-resolved laser flash spectrophotometry with a diffuse reflectance technique.[99] Thus, the excited triplet benzophenone has been shown to be dynamically quenched by naphthalene on silica gel with a diffusion-controlled rate.[100a,b]

Clay interlayers also are useful electrostatic fields for photochemical cyclodimerization. Thus, stilbazolium ions intercalated on montmorillonite interlayers were shown to undergo a selective cyclodimerization to yield a *syn*-HT dimer.[56,57] The high regioselectivity for the *syn*-HT dimer clearly indicates the predominant antiparallel alignment of stilbazolium ions; that is, the stilbazolium ions were alternatively adsorbed on upper and lower layer surfaces of clay, as depicted in Figure 9. In fact, it is known that clay minerals may form a bilayer film of intercalated alkylammonium ions.[101] Interestingly, only excimer fluorescence was observable from clay-intercalated stilbazolium ions in a wide range of 0.1 to 20% coverage. This indicates that the strong excimer fluorescence, even with 0.1% coverage, is realized only through the formation of a cluster of olefin molecules.[102] The cluster formation is supported by the fact that the preferential formation of the *syn*-HT dimer is always observed, regardless of the short coverage, but the adsorbed stilbazolium cations have been realized among particles through an adsorption equilibrium with external bulk solution.[56c]

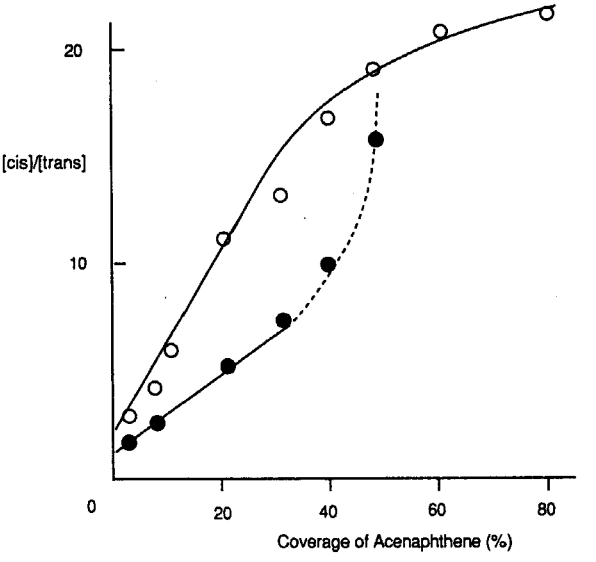

FIGURE 8. Plot of isomer ratio against acenaphthylene coverage: (○) with tumbling and (●) with tumbling in the presence of acenaphthene (total coverage: 1.46 mmol/g of silica gel). (From Bauer, R. K., Borenetein, Jr., deMayo, P., Okada, K., Rafalska, M., Ware, N. R., and Wu, K. C., *J. Am. Chem. Soc.*, 104, 4635, 1982. With permission.)

Another interesting aspect of clay interlayers was revealed by the effect of alkylammonium ions coadsorbed; that is, the clusters of intercalated stilbazolium ions were found to be dissoci-

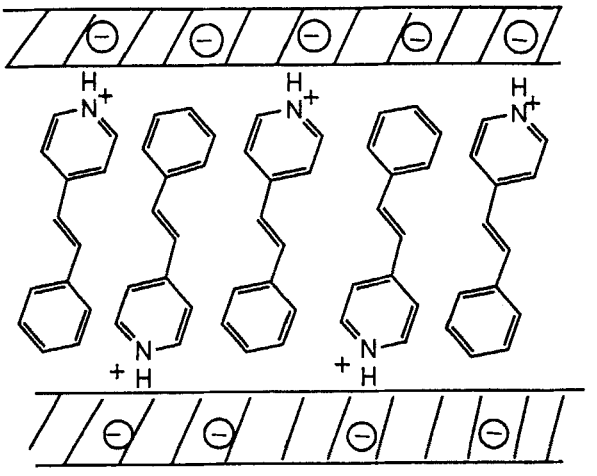

FIGURE 9. A schematic representation of the alkene packing in the interlayers of saponite clay.

ated by adding alkylammonium ions with a molecular length longer than that of the olefin. Coadsorption of long-chain alkylammonium ions effectively quenched the photocyclodimerization of the stilbazolium ion (Figure 10) as well as the excimer fluorescence (Figure 11). Layer distances

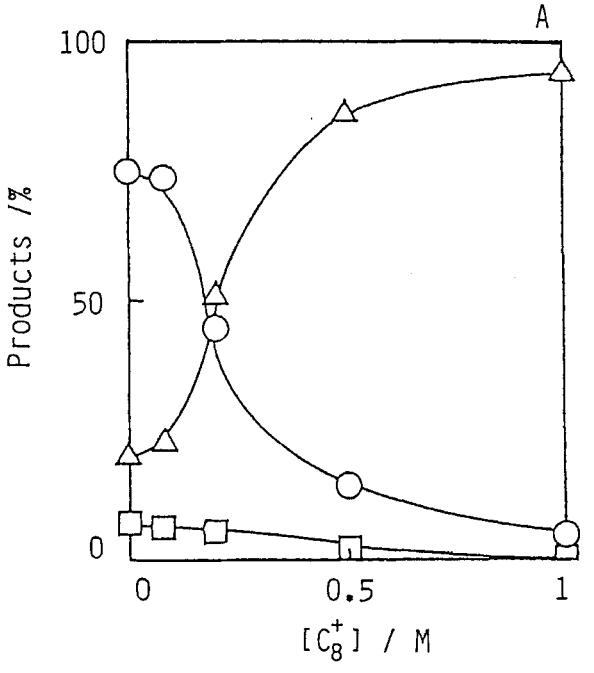

FIGURE 10. Effect octylammonium ions (C_8^+) on photoreactivity of preintercalated stilbazolium ion on clay. -○-:syn head-to-tail dimer; -□-:syn head-to-head dimer; -△-: *cis*-stilbazolium ion.

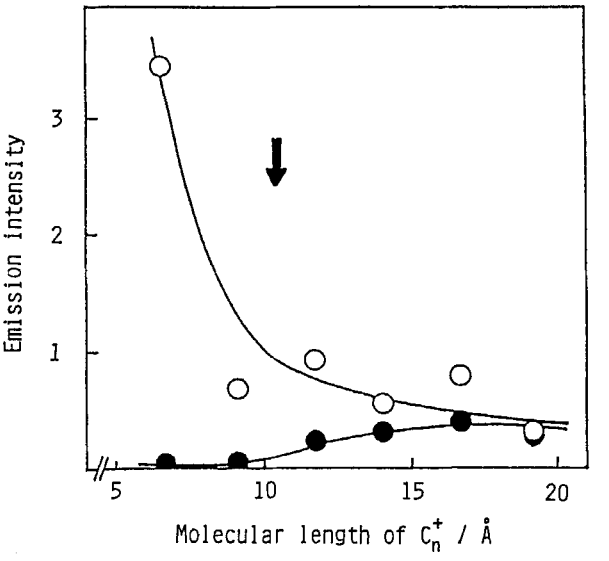

FIGURE 11. Effect of molecular lengths of alkylammonium ion (C_n^+) on the emission of stilbazolium ion intercalated on clay. -○-:excimer fluorescence at 495 nm; -●-:monomer fluorescence at 423 nm.

of the olefin-intercalated clay were estimated by X-ray diffraction analysis to be 9.2 to 9.5 Å, which is somewhat shorter than the molecular length of the olefin, 10.4 Å. The cation-adsorbing sites of the clay were scattered on both sides of the interlayers with average intervals of about 11 Å. Thus, the olefin molecules are adsorbed almost perpendicularly to both surfaces with an alternative stacking, as shown in Figure 9.

Hydrotalcite, an anion-exchanging clay, adsorbs anionically charged olefins such as cinnamate or stilbenecarboxylate anion in its interlayers. The adsorption equilibria are dependent on the kinds of anions. For example, about 37% of the cinnamate anion was intercalated from an equivalent mixture of the clay and cinnamate anion, but stilbenecarboxylate was adsorbed quantitatively. The intercalated carboxylates were photodimerized exclusively to get the corresponding *syn*-HH dimers.[57] Noteworthy here is the lack of *E-Z* photoisomerization, which is in contrast to the reaction in homogeneous solutions. The selective formation of *syn*-HH dimers also indicates the close packing of olefin molecules.

Photocyclodimerization of acenaphthene was found to be susceptible to a space restriction by

the zeolite cavity. When the olefin was irradiated in a cavity of Y-type zeolite with a supercage diameter of 13 Å, the *cis*-cyclodimer (circa 8 Å in diameter) was yielded through an exciplex formation in the cage. The *trans*-cyclodimer (circa 14 Å) is too large to be accommodated in one cavity and is believed to be formed in the cavity linking two supercages, as depicted in Figure 12.[103] The size of the metal cations in the supercage was found to affect the ratio of *cis*- and *trans*-dimers by changing the free volume of the cage.

TABLE 10
Effect of Reaction Media on Photochemical Cycloaddition of Cyclopentenone (59) with Olefins

	Olefin (60)		Yield (%)	
Medium	**R_1**	**R_2**	**61a**	**61b**
Cyclohexane	—	n-C_6H_{13}	53	47
KDC micelle	—	—	88	22
Cyclohexane	OAc	H	25	75
KDC micelle	—	—	51	49
Cyclohexane	—	—	0	100
KDC micelle	—	—	70	30

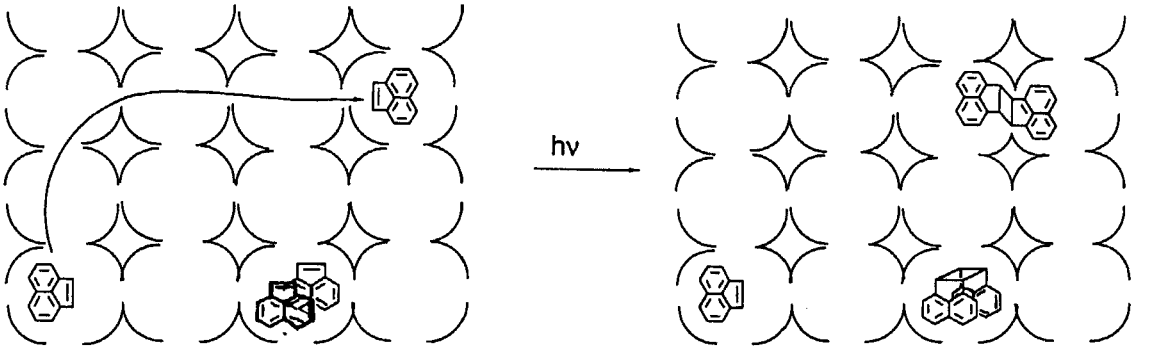

FIGURE 12. Schematic drawings of photocyclodimerization of acenaphthene intercalated in zeolite cavity. (From Ramamurthy, V., Corbin, D. R., Kumar, C. V., and Turro, N. J., *Tetrahedron Lett.*, 31, 47, 1990. With permission.)

2. Crossed Addition

Photochemical crossed additions of olefins are likewise controlled by electrostatic fields. For example, the regiochemistry of the photochemical addition of olefins with cyclopentenone was dependent on the reaction media or micelles.[104a,b] The results are summarized in Table 10. The polar carbonyl groups are directed to the outer interface of KDC micelles and the hydrophobic carbon chains to the inner core. This orientation effect by micelles explains the observed regiochemistry of the adducts.

In the case of a hindered ketone (**62**) adsorbed on silica gel, the photochemical cross addition occurs preferentially on the more hindered side (Equation 28). The stereochemistry was

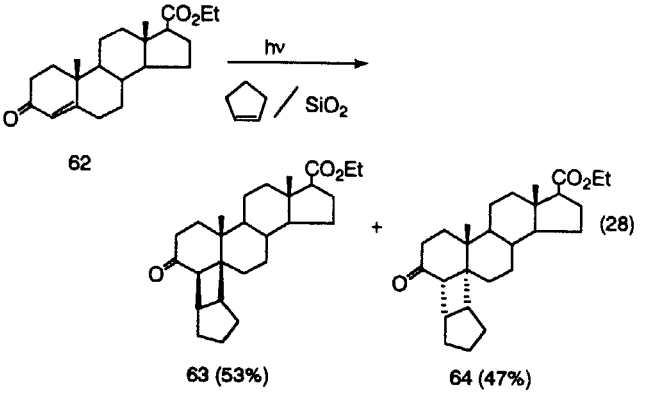

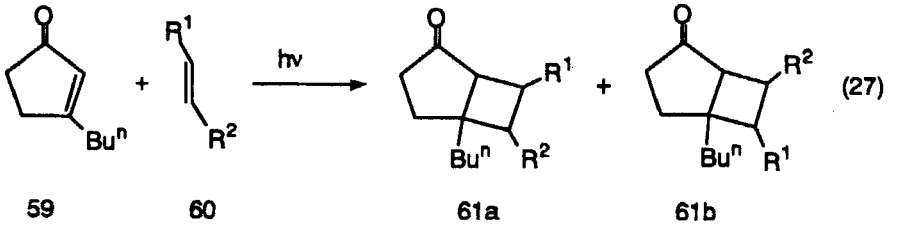

explained by a selective hydrogen bonding of carbonyl with silanol on the silica gel surface from the less hindered side. Thus, the more hindered side of the ketone was open for the attack of cyclopentene.[105,106]

3. Hydrogen Abstractions

Excited triplet ketones take hydrogen atoms from solvent molecules and yield alcohols and/or 1,2-diols. Photolysis of a mixture of SDS and benzophenone-4-carboxylate led to the insertion of the benzophenone carbonyl into the alkyl chain of SDS.[107,108] Detailed product analyses showed that the excited carbonyl randomly attacked the entire chain of SDS from C-5 to C-11. This suggested extensive coiling and folding of the detergent chains in the micelle.

Aromatic ketones covalently bound on silica surface undergo a forced photopinacolization,[109a] as shown in Equation 26, whereas the reaction in micelles causes a crossed adduct between ketones and solvent alcohols.

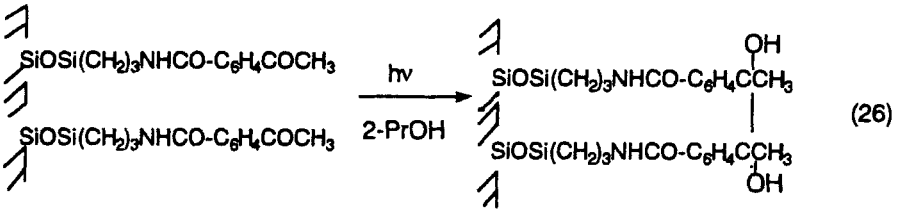

(26)

An optical active sensitizer covalently bonded to a silanol group on the SiO_2 surface, on irradiation, discriminates the chirality of *N, N*-dimethyl-1-phenethylamines as quencher.[109b]

4. Substitutions

Aromatic nitro compounds, such as 4-nitrophenyl alkylesters, 1-nitronaphthalene, and 4-methoxy-1-nitronaphthalene, undergo photochemical substitutions with cyanide ions. The CTAB micelle reportedly increases the quantum yield of the reaction by a factor of about 6800, whereas the SDS micelle strongly inhibits the reaction.[110] The dramatic effect of the CTAB micelle is due to the concentration effect of the cyanide ion on the cationic surface.

The photodecomposition of 4-nitrophenylnitromethane (**67**) is accelerated 67-fold by the presence of a CTAB micelle.[111] This dramatic acceleration was explained by the stabilization of the acinitrate anion by reducing the pK_a value of **67** by 1 pK_a unit. In general, micelles concentrate both substrates and attacking reagents, hence,

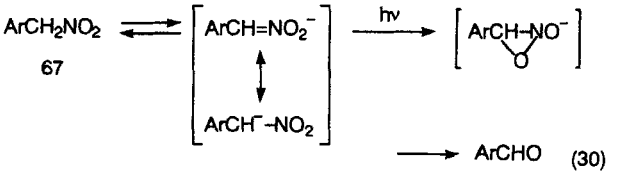

(30)

accelerating the reactions between them. It should be kept in mind, however, that excited lifetimes of substrates are sometimes shortened by the increased polarity of micelle interfaces.[112]

5. Oxidations

Methylene blue (MB)-sensitized photooxidation of styrylketone (**68**) gives rise to oxidatively cyclized products (**69** and **70**) in the presence of SDS micelles. The hydrophobic interior of SDS micelles concentrates the hydrophobic substrate and oxygen, enhancing the reaction of singlet oxygen, an intermediate excited reagent, with **68** in the micelle hydrophobic core.[113]

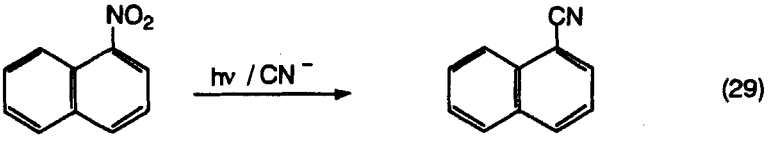

(29)

65 66

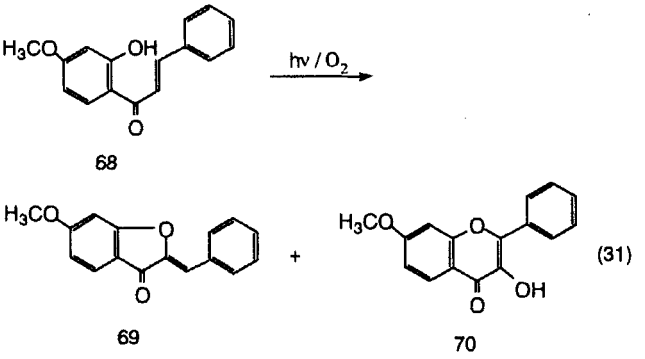

On UV irradiation, 9,10-diethoxyanthracene (**71**) was oxidized by iodonium biphenyl to give ethoxyanthorone (**72**).[114a] One electron oxidation of excited **71**^{*1} by Ph_2I^+ induces the oxygen-carbon

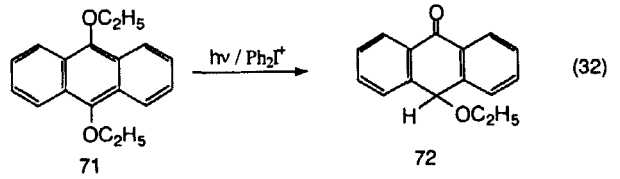

bond homolysis leading to **72.** The reaction was retarded by the addition of AOT reversed micelles. This was because a heavy atom effect of Ph_2I^+ promotes the intersystem crossing of **71**^{*1} to **71**^{*3}, which was followed by rapid picoseconds deactivation to a homolytically dissociation process and, as a result, suppressed the electron transfer between **71**^{*1} and Ph_2I^+.[114b,c] On the other hand, the replacement of Ph_2I^+ with alkyl viologen (RV^{2+}) increased the photooxidation.

C. Energy Transfer Reactions

Energy transfers are important photochemical processes, yielding an excited acceptor (A*) by an excited energy transfer from an excited donor (D*) to A.

$$D^* + A \rightarrow D + A^* \qquad (33)$$

The use of sensitizers is essential in cases in which substrates are not absorbing incident light in suitable UV/visible regions. As described earlier, the photosynthesis centers of plants are composed of a series of light-absorbing chlorophylls, electron mediators, and redox reaction systems that are elaborately organized in a lipid bilayer membrane; the efficient transfer of excitation energy takes place among the antenna chlorophyll in chloroplasts, practically without self-quenching.

Micelles are suitable for constructing efficient energy transfer systems in which D and A pairs can be confined in a small volume of micelle particles. Selective energy transfers between D* and A in SDS and CTAB micelles have been attained because of the high local concentration of D and A.[115a–d]

An elegantly organized energy transfer was studied by Kuhn and Möbius.[20,116a,b] They constructed multilayer assemblies that consisted of oxacyanine (**73**) and thiocyanine (**74**) insulated by pure arachidic acid layers, as shown in Figure 13. Energy transfer from excited **73** to **74** was confirmed at a distance of 50 Å by the observation of a sensitized yellow fluorescence from **74***. The energy transfer was not observed at a longer distance of 150 Å, which was too far for the energy transfer from **73*** to **74.**

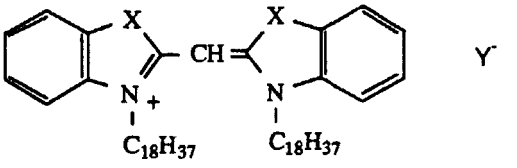

73 (X = O)

74 (X = S)

A systematic study was reported on the dependence of energy-transfer efficiencies on the distance between D* and A. The sophisticated multilayer assemblies were composed of Ru(II)-(2,2′-bipyridine)$_2$(2,2′-bipyridine-4,4′-dicarboxylic acid)$^{2+}$ donor layer (D) and 1,1′-dioctadecyl-4,4′-carbocyanine acceptor layer (A), which were insulated by arachidate spacer layers. The effect of spacer distance, d (Å), on the relative luminescence intensities, I_d/I_∞, of D* was studied, where I_d and I_∞ were the intensities of the ruthenium luminescence in the presence and the absence of A, respectively.[116b] Because the fluorescence maximum of D overlapped with the absorption

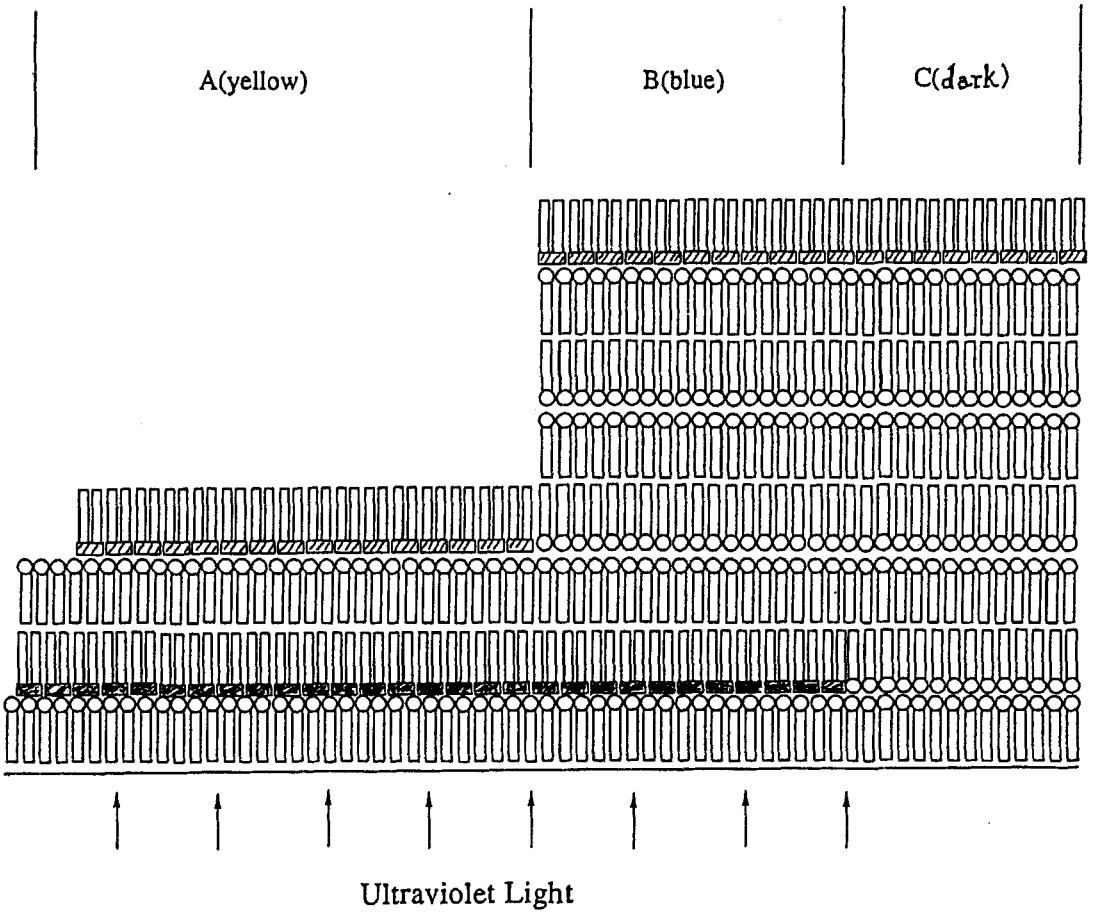

FIGURE 13. Schematic structure of a monolayer assembly with two components consisting of the energy donor (**73,** oxacyanine) and the acceptor (**74,** thiocyanine): a yellow fluorescence from the acceptor in zone (A), a blue fluorescence from the donor in zone (B), and no emissions are observed in zone (C). ▨, **73;** ▩, **74;** ▯, arachidic acid. (From Kuhn, H. and Möbius, D., *Agnew Chem. Int. Ed. Engl.*, 10, 620, 1971. With permission.)

spectrum of A, the Forster-type resonance energy transfer was operative and is expressed theoretically by Equation 34.[117] The relationship between I_d/I_∞

$$I_d / I_\infty = 1 + (d_0 / d)^4 \qquad (34)$$

and d is shown in Figure 14 and clearly suggests that the D*–A energy transfer in this system is of the Forster type.

D. Electron Transfer Reactions

An electron transfer between an excited sensitizer D* and an acceptor A gives rise to a pair of charge separated species, $D^{+\cdot}$ and $A^{-\cdot}$ (Equation 35). The resulting charge separation is to be erased, if no other reactions of $D^{+\cdot}$ and $A^{-\cdot}$ occur, by a rapid back electron transfer to regenerate D and A (Equation 36).

$$D^* + A \rightarrow D^{+\cdot} + A^{-\cdot} \qquad (35)$$

$$D^{+\cdot} + A^{-\cdot} \rightarrow D + A \qquad (36)$$

1. Charge Separations Using Electrostatic Fields

To use the charge-separated species for any chemical reaction, some device must be con-

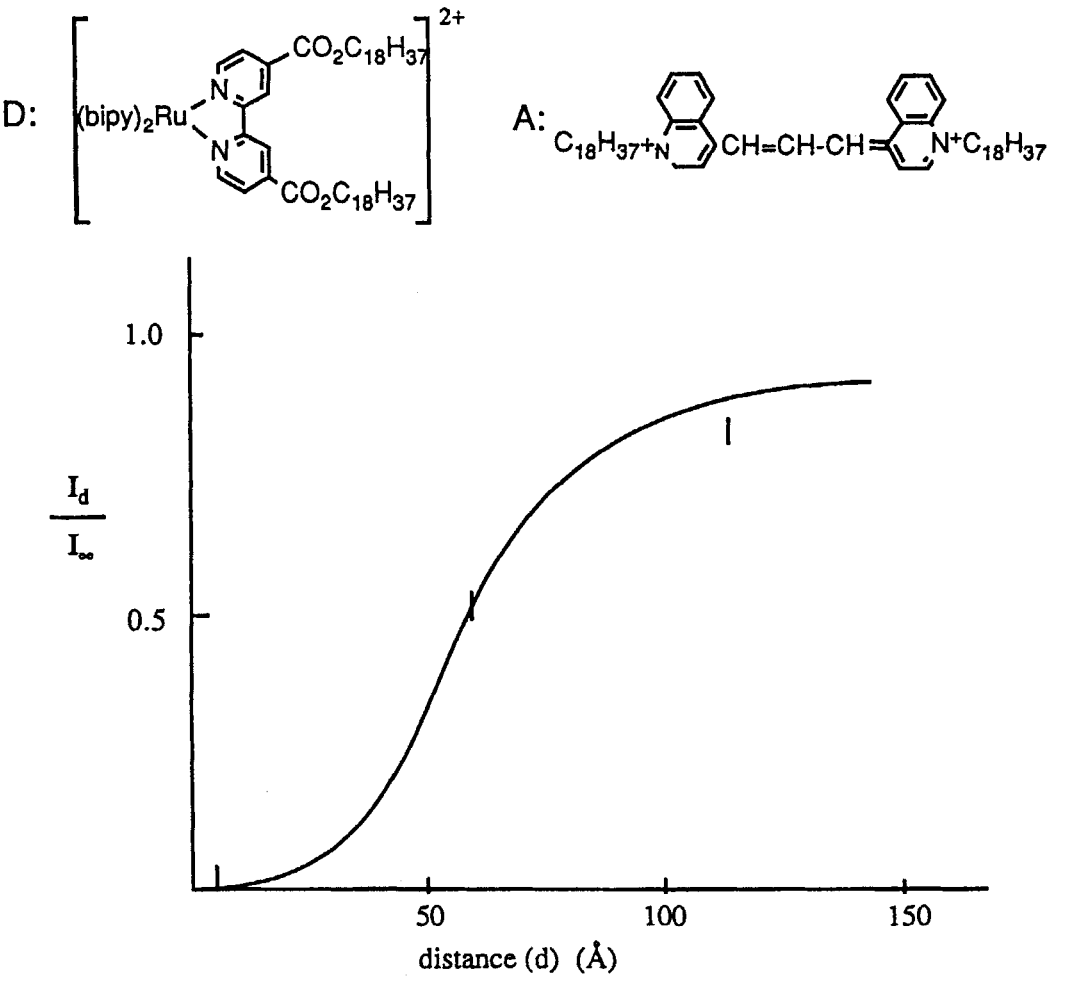

FIGURE 14. Energy transfer in monolayer assembly. A luminescence intensity of D against distance (d) between monolayers D and A. (From Seefeld, K.-P., Möbius, D., and Kuhn, H., *Helv. Chim. Acta,* 60, 2608, 1977. With permission.)

structed to suppress the facile back-electron transfer.[118a,b] Ionic interfaces of micelles are effective devices for such a purpose. A micelle surface forms an electric double layer with a steep electric gradient over a few hundred angstroms. Two mechanisms are envisaged for the stabilization of charge-separated states, as illustrated in Figure 15.[119] When either one of the charge-separated species is repelled from the alike-charged surface, an oppositely charged species interacts strongly with the surface electrostatically, resulting in an effective charge separation [(A) in Figure 15]. An alternative case is shown as B in Figure 15; an isothermic electron relay proceeds among the acceptors series of A_1, A_2, A_3, etc. stabilizing the charge-separated $D^{+\cdot}$ and $A^{-\cdot}$ by the long distance.

A typical example is the dramatic effect of SDS micelles on the photochemical charge separation between zinc(II) tetraphenylporphyrin (ZnTPP) and sodium 2,6-disulfonatoanthraquinone (**75,** R=SO_3Na), eventually yielding sodium 2,6-disulfonatoanthranol (**76,** R=SO_3Na).[120]

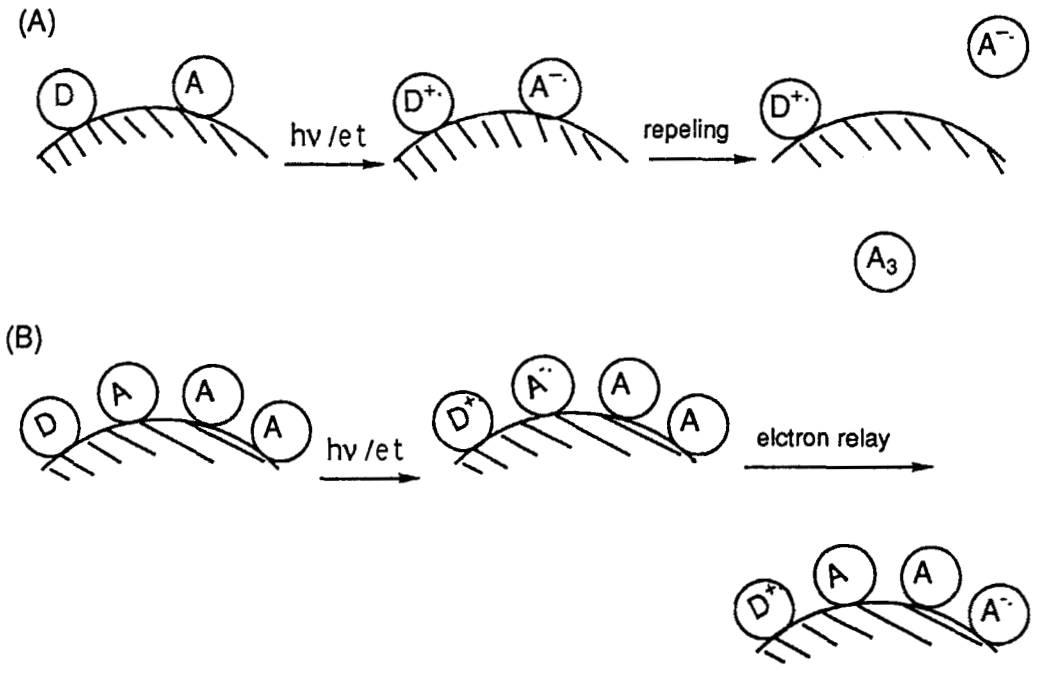

FIGURE 15. Two possible mechanisms for stabilization of a charge-separated species.

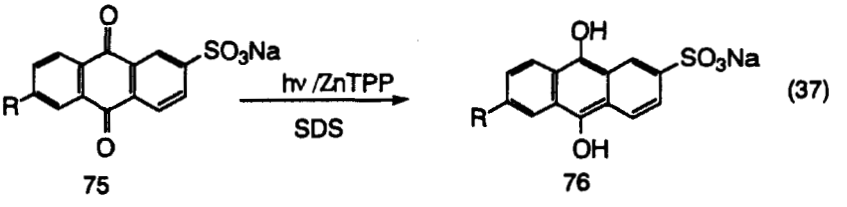

The back-electron transfer is effectively suppressed by the electrostatic repulsion of anion radical **75** from the anionic micelle surface. A similar effect also is noted in the photochemical charge separation between an excited $Ru(bpy)_3^{2+}$ and *N*,*N*′-dimethylaniline[121] or *N*-butylphenotiazine.[122,123] The remarkable effect of micelles has been reported for the charge separation between anthraquinone-2-sulfonate (**75,** R=H) and the hydroxide ion; that is, the addition of CTAB micelles or benzylhexadecyldimethylammonium bromide (BHDB)-reversed micelles accelerates the photochemical one-electron transfer from hydroxide ion to the excited quinone **75***, yielding its anion radical (**75**$^{-}$) or dianion (**75**$^{2-}$).[124] Another effect of the CTAB micelle was reported in the electron transfer between a neutral ZnTPSPyP sensitizer and anthraquinone **75** (R=SO_3Na);[125] the electron transfer becomes possible by dissociating the ZnTPSPyP-quinone complex by the anionic micelle.

A crown ether surfactant (**77**) forms micelle aggregates even in dilute concentrations of $10^{-5} \sim 10^{-3}$ *M*.[126] Such a micelle efficiently accommodates silver ion in its crown ether core. Irradiation of cyanine dye (**78**) in the presence of **77**-Ag^+ micelle leads to a rapid electron transfer within 1.5 ns, giving a micelle-including metallic silver.[127] In this case, the oxidized cyanine dye (78^+) is separated from the reduced silver metal by the micelle aggregate.

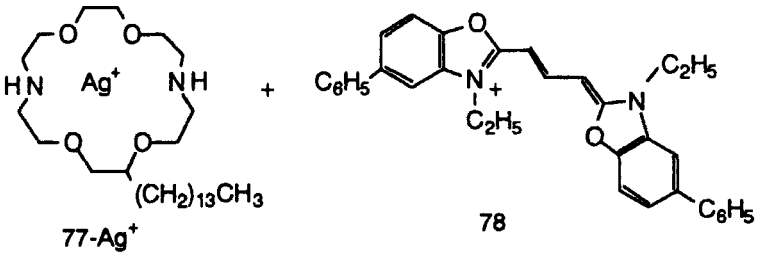

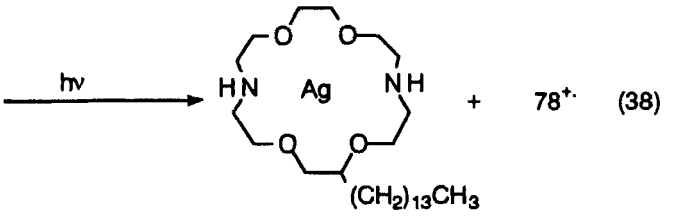

An efficient photoinduced electron transfer has been observed from *N*-methylphenotiazine (**79**) to copper(II) ion incorporated in crown ether micelles.[128] The charge-separated state is accomplished by expelling the resulting cationic **79**$^{+\cdot}$ from the micelle surface. The reduction product is metallic Cu(0), which is stabilized by the crown ether as in the case of 77-Ag(0).

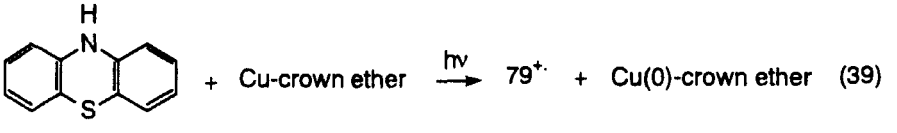

79

Efficient electron transfer reactions can be realized by using redox reagents as counterions of anionic micelles.[129] Thus, copper(II) dodecylsulfate forms a micelle with a cupric ion on the surface. Irradiation of dihydroindol[3, 2-b] ocarbazole (**80**) dissolved in copper(II) dodecysulfate micelle resulted in an effective electron transfer from **80** to cuptic ion.

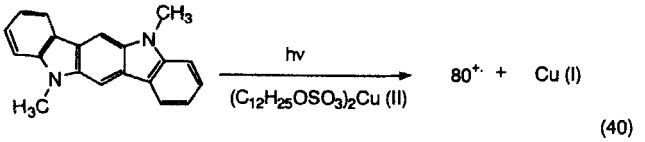

80

Triarylmethane dyes (**81**) bound to polyelectrolytes undergo photochemical electron transfer to alkyl viologen (RV^{2+}) on irradiation. Addition of CTAB micelles in this system increased the population of an excited triplet, a precursor of the electron donor, by a heavy atom effect of the micelle.[130]

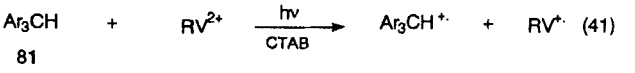

The anionic surface of silica gel also is effective for a charge separation between an excited $Ru(bpy)_3^{2+}$ and a sulfonate viologen (**82**). The sulfonate substituents neutralized the cationic charges on viologen nitrogens and reduced the

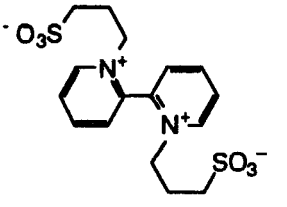

82

electrostatic attraction between **82** and silica gel. When **82** is reduced, the resulting radical (**82**$^{+}$)$\cdot$ is anionically charged and repelled from the sur-

face. The back-electron transfer becomes $10^2 \sim 10^3$ times as slow as that in the absence of silica gel.[131a]

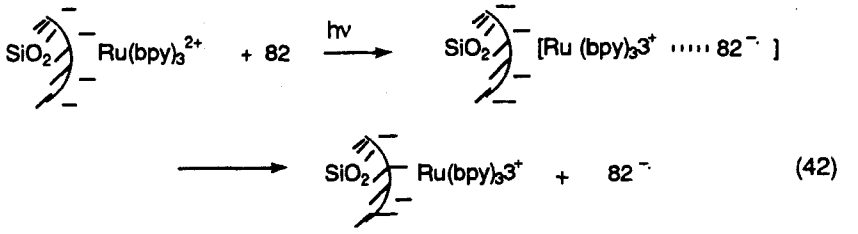

(42)

Photochemical electron-transfer quenching of excited pyrene by *N,N'*-dimethylaniline (DEA) adsorbed on silica surfaces was completely ineffective below the respective DEA monolayer value. Such DEA inertness is interpreted in terms of its strong interaction with surface silanol groups. It is evident that the slopes of Stern-Volmer plots markedly increase above monolayer coverage.[131b]

2. Electron Relays by the Use of Electron Mediators

Viologen with long alkyl chains (**83**) is an excellent electron carrier between aqueous and oil phases. Methyl viologen (MV^{2+}), even after one-electron reduction, is hydrophilic and remains in an aqueous phase. Viologen **83** also is hydrophilic, but its reduced cation radical becomes hydrophobic. Irradiation of Zn(II)TPP or $Ru(bpy)_3^{2+}$ in CTAB micelles, including the surfactant viologen **83,** resulted in a stable charge separation; that is, the reduced viologen **83**$^{+\cdot}$ had a lifetime of several milliseconds.[132] The reduced viologen **83**$^{+\cdot}$ migrated from bulk water to the micelle interior. Thus, a stable charge separation was attained between the excited donor and the electron carrier.

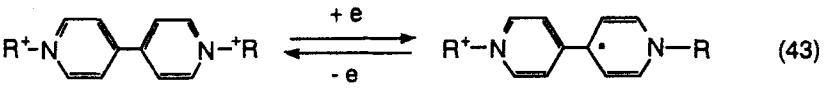

(43)

83, R = $(CH_2)_{13}CH_3$

An interesting photochemical electron pumping system, using alkyl viologens as electron carriers, has been constructed by Tabushi et al., as illustrated in Figure 16.[133] In aqueous phase I, alkyl viologens (RV^{2+}=X) were reduced photochemically by ZnTPPS, which was regenerated by the reaction with sodium thiosulfate. The reduced radical cation X^- transferred into the hydrophobic phase, which, on the opposite side, was in contact with aqueous phase II. Flavin mononucleotide (FMN) dissolved in phase (II) was reduced to FMNH by X^- at the interface with the oil phase. Thus, electrons were simply transferred from aqueous phase I to phase II. It is interesting to note that the efficiency of electron transfer was dependent on the chain length of alkyl viologens, reflecting the hydrophobicity of its reduced form.[134]

When the dioctylbipyridinium ion (C_8V^{2+}) was reduced to its cation radical (C_8V^+) by excited $Ru(bpy)_3^{2+}$, the radical C_8V^+ was shown to yield disproportionately a neutral diradical (C_8V) that is soluble in organic phase (Equation 44b). By using a water-oil two-phase system, in Figure 16, the two-electron reduced viologen was applied to reduce 1,2-dibromides dissolved in phase II.[135]

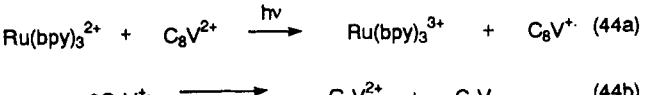

A bilayer membrane of dipalmitoyl-D,L-phosphatidylcholine (DPL) may adsorb $Ru(bpy)_3^{2+}$ and octadecyl viologen ($C_{18}V^{2+}$) on inner and outer interfaces divided by the hydrophobic bilayer. An electron transfer occurred through

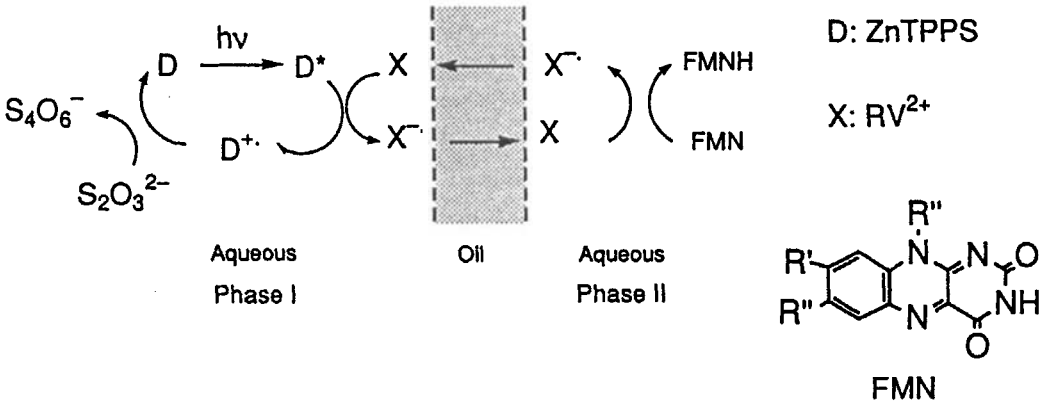

FIGURE 16. Photochemical electron pumping using alkyl viologen as the mediator. (From Tabushi, I., Yazaki, A., Koga, N., and Iwasaki, K., *Tetrahedron Lett.*, 21, 373, 1980. With permission.)

the bilayer membrane to yield a pair of oxidized and reduced species, $Ru(bpy)_3^{3+}$ and $C_{18}V^+$ separated on both sides, the quantum yield being as high as 0.027.[136] A similar charge separation was reported for a pair of $ZnTPyP^+$ and viologens in lipid vesicles.[137,138]

As outlined in Figure 17, concurrent excitation of ZnTPyP adsorbed on both sides of riposome the inner aqueous phase, and the electron was transferred through DBA as a mediator to an another ZnTPyP on the opposite interface. The second step is the photochemical reduction of anthraquinone disulfonate (AQDS) to $AQDSH_2$.[141]

Quinolium salt (**86**) is an excellent mediator for the photoreduction of keto carboxy-

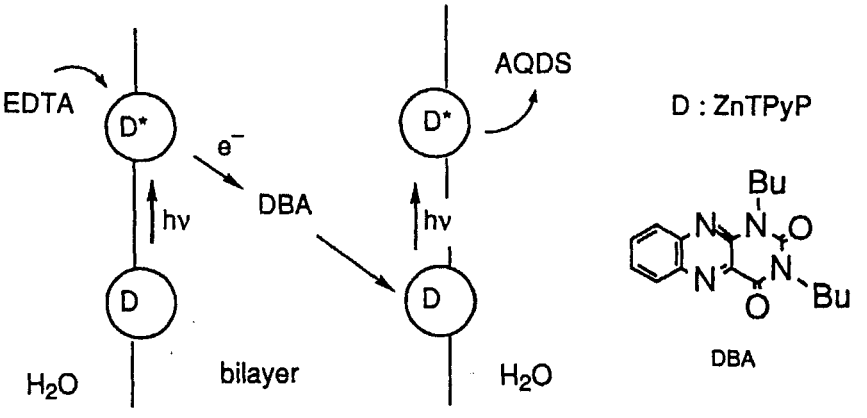

FIGURE 17. Two-step photochemical electron transfer across a bilayer membrane. (From Matsuo, T., Itoh, K., Takuma, K., Hashimoto, K., and Nagamura, T., *Chem. Lett.*, 1009, 1980. With permission.)

bilayer interfaces is an elegant model system of an electron transfer reaction mimicking photosynthesis.[139,140] In the photochemical electron transfer across the bilayer membrance, excited ZnTPyP was reduced by EDTA (ethylene diamine tetraacetic acid) in lates.[142] That is, the photochemical reduction of methyl benzoylformate (**84**) to α-hydroxyphenylacetate (**85**) was attained by using ZnTPPS sensitizer and quinolinium amide **86** as the electron mediator. The iradiation of a mixture of **84**, ZnTPPS, and **86** in the presence

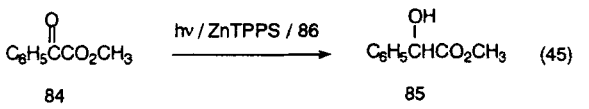

of CTAB micelles resulted in the formation of α-hydroxyacetate **85.** In this case, mediator **86** was solubilized in the hydrophobic core of CTAB micelles, but anionically charged ZnTPPS was

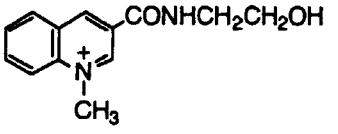

86

in the bulk water because of the electrostatic repulsion with the micelle surface. As depicted in Figure 18, the quinolinium salt **86** carried electrons efficiently from the micelle surface to the hydrophobic interior via the reduced form **87.**

A photochemical ejection of electrons has been observed in the case of surfactantized phenothiadine (**88** R=$(CH_2)_{12}SO_3Na$). On UV il-

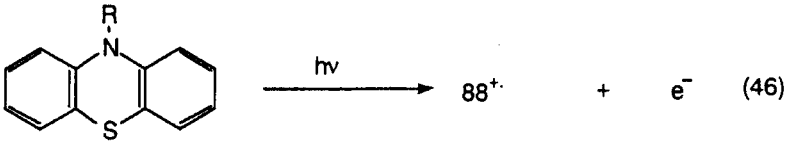

88 (R=$(CH_2)_{12}SO_3Na$)

lumination, the surfactant molecules ejected electrons to give cation radical **88**$^{+\cdot}$, which was significantly stable with a lifetime of a few days.[143a–c]

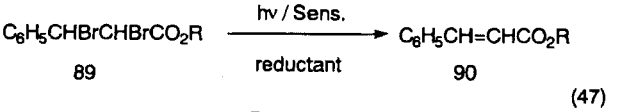

a, R = H; b, R = Na

Sens.: ZnTPP, ZnTPPS

Debromination was initiated by a one-electron transfer from the sensitizer to **89** by de-

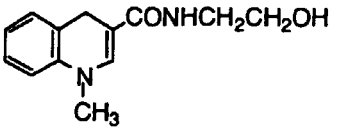

87

tecting a transient ZnTPP(S)$^+$ by laser flash spectroscopy. In addition, the following characteristics were noted in the reaction: (1) radical species were intervened during the sequence because a controlled reaction in toluene yielded diphenylethane and benzylbromide at the expense of cinnamic acid; and (2) the quantum yields for the formation of **90** exceeded unity, implying the occurrence of radical chain reactions. Debromination may be described as the following reaction sequences.

3. Some Electron-Transfer-Induced Reactions

The effect of micelles has been studied on the photochemical debromination of 2,3-dibromocinnamic acid (**89**) with suitable reductants and sensitizers.[144] ZnTPP was used as a hydrophobic sensitizer and its sulfonate (ZnTPPS) as an anionic sensitizer. EDTA or triethanol amine (TEtOA) was used as the reductant.

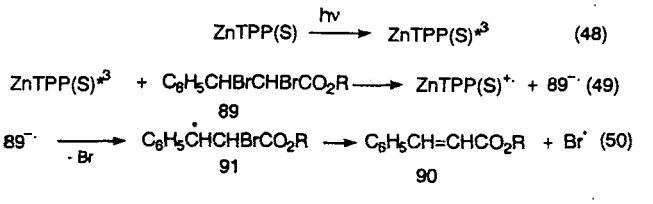

$$ZnTPP(S)^{+\cdot} \xrightarrow{N(CH_2R)_3} ZnTPP(S) + \underset{92}{N(CH_2R)_3^{+\cdot}} \quad (51)$$

$$92 \longrightarrow \underset{93}{(RCH_2)_2\dot{N}CHR} + H^+ \quad (52)$$

$$89 + 93 \longrightarrow 89^{\cdot-} + (RCH_2)_2N^+{=}CHR \quad (53)$$

Table 11 shows the effect of CTAB on debromination efficiencies of **89.** The most effective was system S→S, where both ZnTPPS and **89b** were adsorbed on the anionic micelle interface; and the most ineffective was system I→I, where ZnTPP and **89a** were in the micelle interior. System S→S was about 14 times as efficient as I→I. Intermediate efficiencies were observed in the case of system S→I or I→S, where the sensitizer and dibromide **(89)** were separately dissolved either in the interface or the interior.[9]

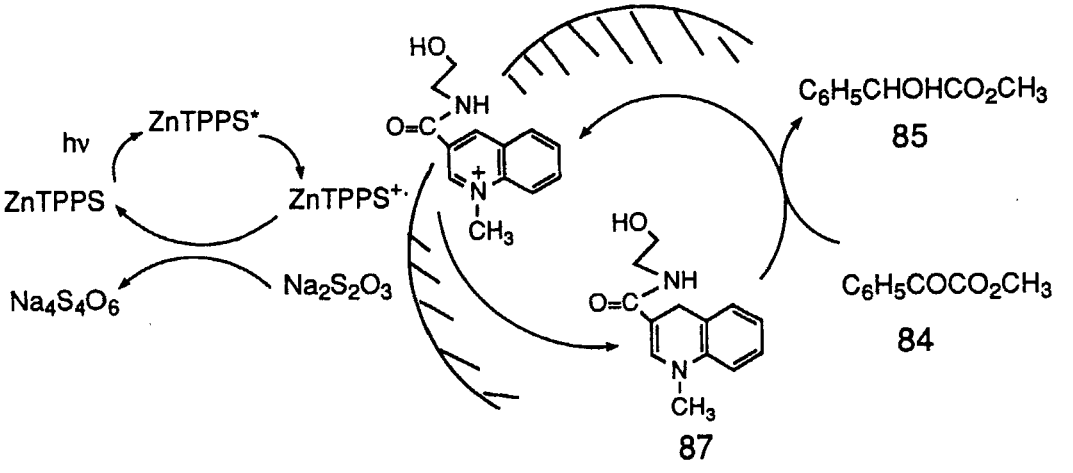

FIGURE 18. ZnTPPS-sensitized reduction of methyl benzoylformate **(84)** to methyl α-hydroxylphenylacetate **(85)** in CTAB micelle, mediated by quinolilium ion **(86).** (From Tabushi, I., Kugimiya, S., and Mizutani, T., *J. Am. Chem. Soc.*, 105, 1658, 1983. With permission.)

TABLE 11
Debromination of 2,3-Dibromocinnamic Acid (89) Sensitized by ZnTPP or ZnTPPS in Micelles

Sensitizer	Acceptor/reductant[a]	Surfactant	System[b]	Formation of 90 (Φ)
ZnTPP	**89a** (R=H)/EDTA	CTAB	I→I	0.04
ZnTPP	**89a** (R=H)/TEOA	SDSme[c]	I→I	0.01
ZnTPP	**89b** (R=Na)/EDTA	CTAB	I→S	0.28
ZnTPPS	**89a** (R=H)/EDTA	CTAB	S→I	0.36
ZnTPPS	**89b** (R=Na)/TEOA	CTAB	S→S	1.39

[a] EDTA = ethylenediaminetetraacetic acid; TEOA = triethanolamine.
[b] Notation of system is described in the text.
[c] SDSme: a mixture of SDS (10 m*M*), amylalcohol (61 m*M*), and dodecane (16 m*M*).

Overall quantum yields for debromination are correlated with the efficiencies of a net charge separation between sensitizer and **89.** The superiority of S→S over other systems can be explained by the following points: (1) the back-electron transfer was slowed by the charge separation of $ZnTPP(S)^{+\cdot}$ and 89^{-} on the electrostatic field of the CTAB micelle; (2) the accompanying attraction was weakened by the neutralization of the net charge with the anionic surfactant.

Another method to separate an oxidized species from a reduced one is shown in Figure 15B. A typical example is a $Ru(bpy)_3^{2+}$-sensitized *cis*- to-*trans*-isomerization of stilbazolium ions adsorbed on SDS micelles.[29] It was concluded that the *cis*-to-*trans* one-way isomerization proceeded via pyridyl radicals formed by photochemical one-electron reductions. Noteworthy here is the high quantum yield for the isomerization in the presence of SDS. Table 12 summarizes the variable quantum yields with the types of micelles used. Most interesting in Table 12 is the fact that the resulting quantum yields were practically the same with the N_A of the anionic micelles; that is, all the molecules adsorbed on a micelle underwent the *cis*-to-*trans*-isomerization by only one photon. This indicates an electron-relay chain reaction (Equations 54 and 55) on the micelle surface, as illustrated in Figure 19.

Poly(styrenesulfonate) anion provides a polyanionic field with a wide range of 100 to 5000 anionic sites, which are expected to form much larger molecular aggregates of *cis*-stilbazolium ions. In fact, sodium poly(styrenesulfonate), with a degree of polymerization of 5000, was shown to gather about 4300 molecules of **94** on its polymer chain. However, the observed quantum yields for the isomerization were not as high as those expected from the degree of polymerization.[145] The quantum yields were always around 100, irrespective of the size of the aggregates. These almost constant quantum yields suggest a formation of clusters similar to micelles. The electron relay would be confined in one cluster with N_A of about 90 (Table 13).

The same *cis*-to-*trans*-isomerization of *cis*-**94** also takes place on silica colloid surfaces with a quantum efficiency more than unity. Because the adsorption of olefins caused the precipitation of colloids, it was impossible to adsorb the olefins sufficiently to induce an efficient electron relay reaction.[146]

Clay interlayers are sometimes used for photochemical charge separation.[147,148] Thus, $Ru(bpy)_3^{2+}$-sensitized electron transfer occurs in the presence of methyl viologen, MV^{2+}, triethanolamine, and clay colloids. Reduced viologen radical cations donate an electron to the proton, yielding molecular hydrogen (Equation 56).

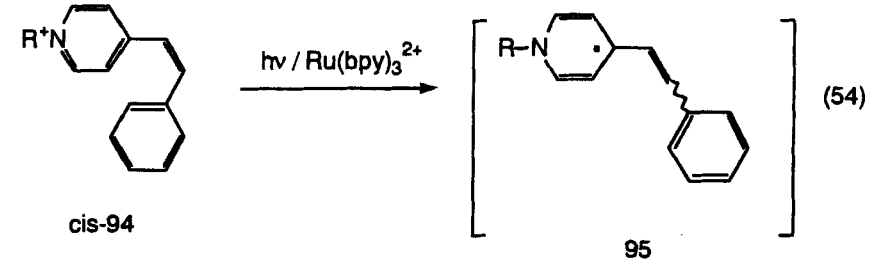

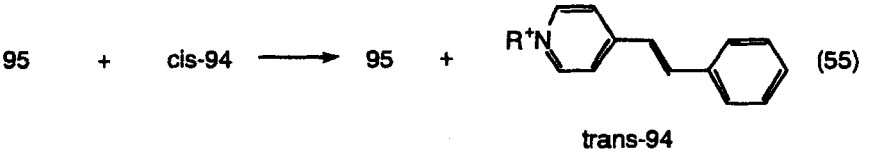

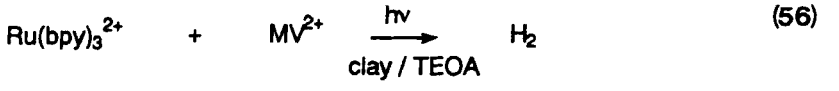

TABLE 12
Limiting Quantum Yields $(\Phi_{c\to t})_{max}$ for the Isomerization of *cis*-94 in Various Surfactant Systems[a]

Surfactant	$(\Phi_{c\to t})_{max}$	Aggregation number N_A^0	Aggregation number N_A
None	0.5 ± 0.03		
Sodium dodecyl sulfate (SDS)	64 ± 2 (63)	62	70
Sodium decyl sulfate (SDeS)	49 ± 1	50	60
Sodium tetradecyl sulfate (STS)	86 ± 4	82	
SDS microemulsion	98 ± 9	100	113
DTAB[b]	0.73 ± 0.05	50	

[a] Conditions: $[Ru(bpy)_3^{2+}]$ 7.7×10^{-6} to 9.7×10^{-5} *M*; [surfactant], 1.8 to 6.0 $\times 10^{-3}$ *M*; [*cis*-**94**] 2.0 to 7.2×10^{-3} *M*.
[b] Dodecyltrimethylammonium bromide.

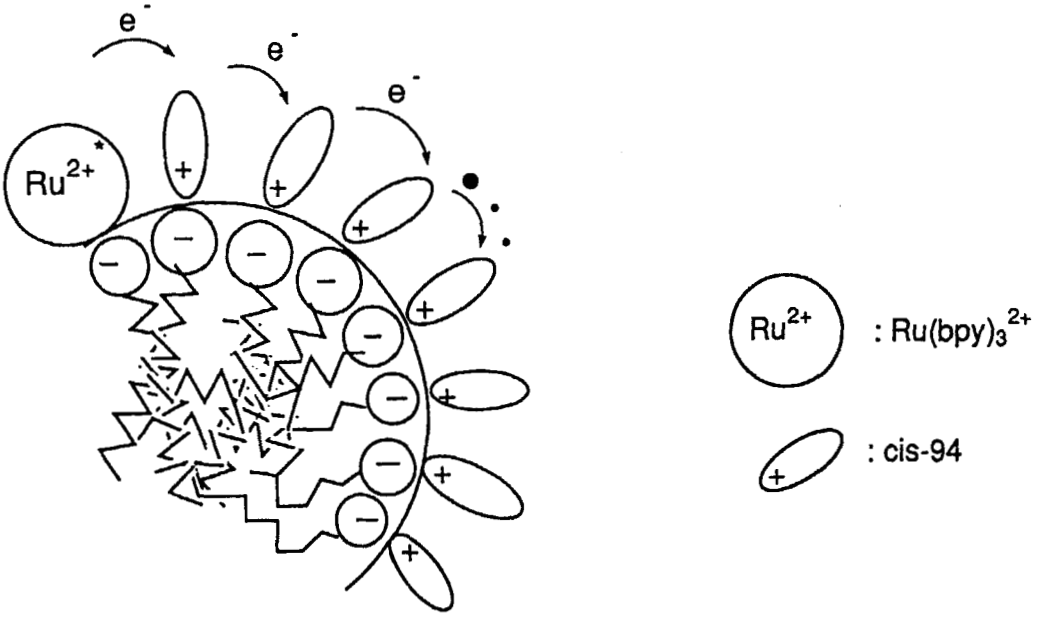

FIGURE 19. Schematic picture for the electronic-relay chain reaction.

An efficient charge-separation was observed when the sensitizer and methyl viologen were adsorbed separately on different interlayers.[149] The separated adsorptions may be attained on the basis of different ion densities on every layer.[150] Hydrogen generation was also observed using Cu^{2+}, Eu^{2+}, nitrobenzene, and dimethylanilinium ion as electron acceptors.[151] It is noted here that these acceptors diffuse into the clay interlayers at rates close to those observed in homogeneous solutions.[56c]

A remarkably enhanced decomposition of water was observed on irradiation of a mixture of $Ru(bpy)_3^{2+}$-adsorbed sepiolite clay and Eu^{2+}-coated aluminum hydroxide in water when RuO_2 and platinum colloid were coated on the sepiolite clay, respectively.[152,153]

TABLE 13
Adsorption and Aggregation Numbers of *cis*-94 Cation on PSS^{n-} Anion and the Quantum Yields ($\Phi_{c\to t}$) for $Ru(bpy)_3^{2+}$-Sensitized Isomerization of *cis*-94 in Water

	Polystyrenesulfonate, $_{PSS}^{n-}$				$\Phi_{c\to t}$	
No.	Mol. weight	Polymer degree *(n)*	Adsorption no.	Aggregation no. (N_A)	1/1	3/1
1	None				1.1	
2	SDS			70	64	
3	2×10^4	100	82 (82%)		51	84
4	7×10^4	360	342 (95%)	93	60	93
5	3.5×10^5	1700			44	107
6	5×10^5	2400	2140 (89%)	78	44	119
7	1×10^6	4900	4800 (90%)	74	66	110
8	1.06×10^6	5100	4350 (87%)	79	58	106

Zeolites are used as templates for organizing photochemically active molecules in a photochemical electron transfer involving $Ru(bpy)_3^{2+}$ and MV^{2+}. On irradiation of trapped $Ru(bpy)_3^{2+}$, MV^+ was formed in neighboring cages that was stable on the hour-time scale.[154a,b] As a more improved system for photochemical electron transfers, the following diad system, D-S-A, has been presented. By intercalating a ruthenium complex (**96**) with a covalently bound viologen-like acceptor (DQ^{2+}), the DQ^{2+} moiety was inserted into the cavity of zeolite, keeping the RuL_3^{2+} moiety out in the bulk.[155]

zeolite resulted in the charge-separated state of less than 100 ns. The charge separation of the longer lifetime was accomplished through the efficient electron relay from the reduced $DQ^{+\cdot}$ to BV^{2+} molecules incorporated in the zeolite cavity.

Hydrogen evolution has been observed in the case of xenthene and MV^{2+} paired on a silica colloid surface,[156] which is similar to the previous example of an efficient charge separation between excited $Ru(bpy)_3^{2+}$ and anionic electron acceptor **82** (Equation 42).

Potassium niobate, $K_4Nb_6O_{17}$, is a layer-structured compound that includes hydrated and

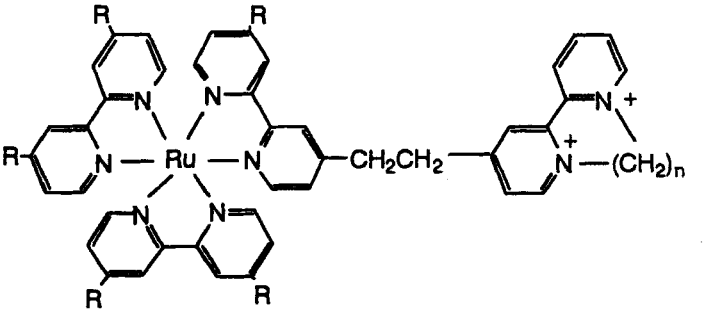

96 (R = H and CH_3; n = 2-3) $[RuL_3^{2+}$— 2DQ]

Irradiation of **96** with zeolite, having benzyl viologen (BV^{2+}, B—$PhCH_2$ in **83**) in zeolite cavities, resulted in the efficient charge separation between **96** and BV^{2+}. As shown in Figure 20, the charge-separated species persisted for 37 ms, whereas a control experiment without the unhydrated potassium ions in every other layer. Irradiation of methyl viologen intercalated in the layer gave rise to the stable cation radical MV^{2+}, which lasted a few days.[157–159]

Zeolite cavities are potentially useful for the immobilization of reactive intermediates that are

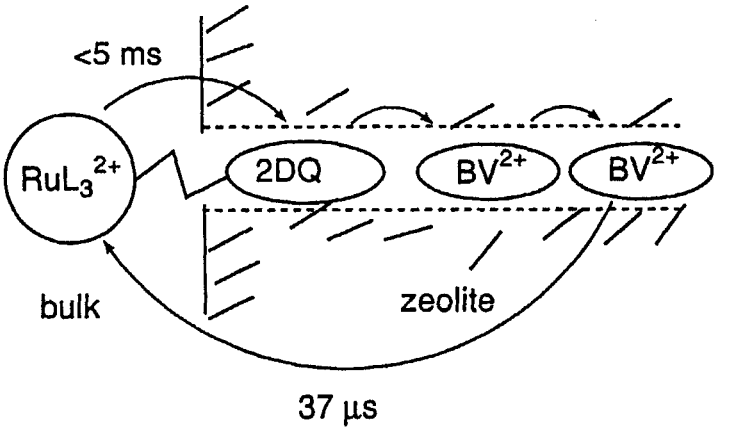

FIGURE 20. The efficient charge separation of **96** in a zeolite cavity. (From Krueger, J. S., Mayer, J. E., and Mallouk, T. E., *J. Am. Chem. Soc.*, 110, 8232, 1988. With permission.)

otherwise subject to rapid diffusive annihilation in solution. The stabilization of the radical cation MV^{2+} is much improved in a cavity of zeolite Y. The introduction of molecular oxygen resulted in quenching of the zeolite-trapped viologens, but the subsequent evacuation of oxygen retrieved the blue color of the cation radical when **98** was used (Equation 57).[160] The redox process was retrievable more than 10 times. Superoxide anion $O_2^{-\cdot}$ formed on silica gel has been studied using EST techniques.[161]

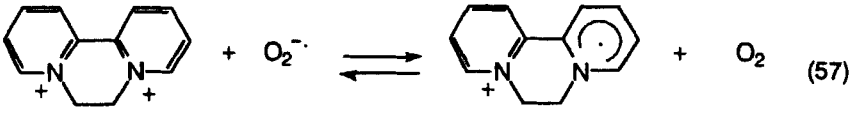

98 $98^{-\cdot}$

IV. SCOPE OF ELECTROSTATIC REACTION FIELDS

The various kinds of reaction fields described here include interfaces that adsorb or accommodate photoreactive compounds and sometimes organize them into a geometrically arranged conformation. Such a sterically controlled system, in contrast to solution photochemistry, may provide unique photochemical reactivities characteristic of molecular arrangements. The electrostatic fields also are suitable for developing an efficient photochemical charge separation, mimicking photosynthesis by plants. It is certain that further developments of sophisticated reaction fields may provide new fields in photochemistry and photobiology.

ACKNOWLEDGMENT

The authors are grateful to Mr. Morio Inaishi for preparing the manuscript.

REFERENCES

1. **Fendler, J. H.,** *Membrane Mimetic Chemistry*, Wiley-Interscience, New York, 1982, 6.
2. **Hartley, G. S.,** State of solution of colloidal electrolytes, *Quart. Rev. Chem. Soc.*, 2, 152, 1948.
3. **Verbeck, A., Gelade, E., and DeSchryver, F. C.,** Aggregation behavior in inversed micellar systems: spectroscopic evidence for a unified model, *Langmuir*, 2, 448, 1986.
4. **Kalyanasundaram, K. and Thomas, J. K.,** Environmental effects on vibronic band intensities in pyrene monomer fluorescence and their application in studies of micelle system, *J. Am. Chem. Soc.*, 99, 2039, 1977.

5. **Otruba, J. P. and Whitten, D. G.** Solubilization in detergent micelles: "interactive" nature of the solubilization process as indicated by a study of intermolecular charge-transfer complexes, *J. Am. Chem. Soc.*, 105, 6503, 1983.
6. **Bonilha, J. B. S., Foreman, T. K., and Whitten, D. G.,** Hydrophobic and entropic factors in the solubilization of ionic substrates in micelles, *J. Am. Chem. Soc.*, 104, 4215, 1982.
7. **Kunjappu, J., Somasundaram, P., and Turro, N. J.,** A luminescence quenching study on the location problem of $Ru(bpy)_3^{2+}$ in micelles and hemimicelles, *J. Phys. Chem.*, 94, 8464, 1990.
8. **Rodgers, M. A. and Baxendale, J. H.,** Fluorescence of tris(2,2′-bipyridine)-ruthenium(II) in sodium dodecylsulfate solutions below the critical micelle concentration, *J. Phys. Chem.*, 86, 4906, 1982.
9. **Takagi, K., Miyake, N., Nakamura, E., Usami, H., and Sawaki, Y.,** Micellar effect on the photosensitized debromination of 2,3-dibromo-3-phenylpropionic acid, *J. Chem. Soc. Faraday Trans. 1*, 84, 3475, 1988.
10. **Hashimoto, S. and Thomas, J. K.,** Luminescence quenching in NaLS micellar system at 77K, *J. Am. Chem. Soc.*, 105, 5230, 1983.

11a. **Fendler, J. H., Fendler, E. J., Medary, R. T., and ElSeoud, O. A.,** Proton magnetic resonance investigations of the formation of allyl propionate micelles in benzene and in carbon tetrachloride, *J. Chem. Soc. Faraday Trans. 1*, 69, 280, 1973.

11b. **Fendler, E. J., Fendler, J. H., Medary, R. T., and ElSeoud, O. A.,** Proton magnetic resonance investigations of alkylammonium carboxylate micelles in nonaqueous solvents, *J. Phys. Chem.*, 77, 1432, 1973.

12. **Eriksson, J. C.,** NMR-experiments on solubilization in soap micelles, *Acta Chem. Scand.*, 17, 957, 1967.
13. **Turro, N. J. and Yekta, A.,** Luminescent probe for detergent solutions. A simple procedure for determination of the mean aggregation number of micelles, *J. Am. Chem. Soc.*, 100, 5951, 1978.

14a. **Turro, N. J., Grätzel, M., and Braun, A. M.,** Photophysical and photochemical processes in micellar systems, *Angew. Chem. Int. Ed. Engl.*, 19, 675, 1980.

14b. **Imae, T. and Kohsaka, T.,** Size and electrophoretic mobility of C_{14}TASal micelles in aqueous media, *J. Phys. Chem.*, 96, 10030, 1992.

15. **Fuhrhop, J. H. and Mathieu, J.** Routes to functional vesicle membranes without proteins, *Angew. Chem. Int. Ed. Engl.*, 23, 100, 1984.

16a. **Lianos, P., Mukhopadhyay, A. K., and Georghiou, S.,** Microenvironment of aromatic hydrocarbons employed as fluorescent probes of liposomes, *Photochem. Photobiol.*, 32, 415, 1980.

16b. **Georghiou, S. and Mukhopadhyay, A. K.,** Phase transitions and cholesterol effects in phospholipid liposomes. A new method employing the enhancement of the 0,0 vibronic transition of pyrene, *Biochim. Biophys. Acta*, 645, 365, 1981.

17. **Suddaby, B. R., Brown, P. E., Russell, J. C., and Whitten, D. G.,** Surfactant and hydrophobic derivatives of trans-stilbenes as probes of vesicle and micelle solubilization sites. Studies using fluorescence and photoisomerization as probes, *J. Am. Chem. Soc.*, 107, 5609, 1985.
18. **Mizutani, T. and Whitten, D. G.,** Evidence for wide variation of solubilization/reaction sites in microheterogeneous media, *J. Am. Chem. Soc.*, 107, 3621, 1985.
19. **Schanze, K. S., Shin, D. M., and Whitten, D. G.,** Micelle and vesicle solubilization sites. Determination of micropolarity and microviscosity using photophysics of a dipolar olefin, *J. Am. Chem. Soc.*, 107, 507, 1985.

20a. **Kuhn, H., Möbius, D., and Bucher, H.,** Spectroscopy on monolayer assemblies. I. Principles and applications. II. Experimental procedure, in *Physical Methods of Chemistry*, Vol. 1, Weissberger, A. and Rossiter, B. W., Eds., Wiley-Interscience, New York, 1972, 577.

20b. **Kuhn, H. and Möbius, D.,** Systems of monomolecular layers. Assembling and physicochemical behaviors, *Angew. Chem. Int. Ed. Engl.*, 10, 620, 1971.

21a. **Quina, F. H. and Whitten, D. G.,** Medium effects on photochemical reactions. Photochemistry of surfactant alkyl 4-stilbazole salts in solution, in the solid state, and in monolayer assemblies, *J. Am. Chem. Soc.*, 97, 1602, 1975.

21b. **Sprintschnik, G., Sprintschnik, H. W., Kirsch, P. P., and Whitten, D. G.,** Preparation and photochemical reactivity of surfactant ruthenium(II) complexes in monolayer assemblies and at water-solid interfaces, *J. Am. Chem. Soc.*, 99, 4947, 1977.

22a. **Hayakawa, K. and Kwak, J. C. T.,** Surfactant-polyelectrolyte interactions. I. Binding of dodecylcetyltrimethylammonium ions by sodium dextran and sodium poly(styrene-sulfonate) in aqueous solution in the presence of sodium chloride, *J. Phys. Chem.*, 86, 3866, 1982.

22b. **Hayakawa, K. and Kwak, J. C. T.,** Surfactant-polyelectrolyte interactions. II. Effect of multivalent counterions on the binding of dodecyltrimethylammonium ions by sodium dextran sulfate and sodium poly(styrenesulfonate) in aqueous solutions, *J. Phys. Chem.*, 87, 506, 1983.

23. **Malovikova, A., Hayakawa, K., and Kwak, J. C. T.,** Surfactant-polyelectrolyte interactions. IV. Surfactant chain length dependence of the binding of allylpyridinium cations to dextran sulfate, *J. Phys. Chem.*, 88, 1930, 1984.
24. **Hayakawa, K. and Kwak, J. C. T.,** Cooperative binding of ionic surfactants by polyelectrolytes, *Hyomen (Surface)*, 23, 169, 1985.
25. **Turro, N. J.,** Luminescence probes for the investigation of the structure and dynamics of aqueous solutions of micelles and related systems, *Gov. Rep. An-*

nounce. Index, 86, 646661, 1986 (*Chem. Abstr.*, 106, 73345h, 1987).
26. **Chu, D.-Y. and Thomas, J. K.,** Photophysical and photochemical studies on a polymeric intermolecular micellar system, PA-18K_2, *Macromolecules,* 20, 2133, 1987.
27. **Turro, N. J. and Arora, K. S.,** Pyrene as a photochemical probe for intermolecular interactions of counter-soluble polymer in dilute solution, *Polymer,* 27, 783, 1986.
28. **Chu, D.-Y. and Thomas, J. K.,** Effect of cationic surfactants on the conformational transition of poly(methacrylic acid), *J. Am. Chem. Soc.*, 108, 6270, 1986.
29. **Takagi, K., Aoshima, K., Sawaki, Y., and Iwamura, H.,** Electron-relay chain mechanism in the sensitized photoisomerization of stilbazol salts in aqueous anionic micelles, *J. Am. Chem. Soc.*, 107, 47, 1985.
30. **Turro, N. J. and Kuo, P.-L.,** Photoluminescence probes for pressure and temperature effects on the aggregates of water-soluble block copolymers, *J. Phys. Chem.*, 90, 4205, 1986.
31. **Strauss, U. P. and Vesnaver, G.,** Optical probes in polyelectrolyte studies. II. Fluorescence spectra of dansylated copolymers of maleic anhydryde and alkyl vinyl ethers, *J. Phys. Chem.*, 79, 2426, 1975.
32. **Bedner, B., Morawetz, H., and Shafer, J. A.,** Kinetics of the cooperative complex formation and dissociation of poly(acrylic acid) and poly(oxyethylene), *Macromolecules,* 17, 1634, 1984.
33. **Delaire, J. A., Rodgers, M. A. J., and Webber, S. E.,** Quenching of fluorescence in water-soluble copolymers of methacrylic acid and vinylphenylanthracene, *J. Phys. Chem.*, 88, 6219, 1984.
34. **Roland, B. and Smid, J.,** Clustering of hydrophobic ions in the presence and absence of the polysoap poly(vinylbenzo-18-crown-6), *J. Am. Chem. Soc.*, 105, 5269, 1983.
35. **Wong, K.-H., Kimura, K., and Smid, J.,** Fluorescence of auramine O and its binding to poly(vinylbenzo-18-crown-6) and to polyvinylbenzoglyme in water, *J. Poly. Sci.: Poly. Chem. Ed.*, 21, 579, 1983.
36. **Synder, L. R. and Ward, J. W.,** The surface structure of porous silica, *J. Phys. Chem.*, 70, 3941, 1966.
37. **Oelkrug, D., Flemming, W., Fullemann, R., Gunther, R., Honnen, W., Krabichler, G., Shafer, M., and Uhl, S.,** Photochemistry on surfaces, *Pure Appl. Chem.*, 58, 1207, 1986.
38. **Turro, N. J.,** Photochemistry of ketones adsorbed on porous silica, *Tetrahedron,* 43, 1589, 1987.
39a. **Theng, K. G.,** *The Chemistry of Clay-Organic Reactions,* Adam Hilger, London, 1974.
39b. **Grim, R. E.,** *Clay Mineralogy,* McGraw-Hill, New York, 1953.
40. **Barrer, R. M.,** Shape-selective sorbents based on clay minerals: a review, *Clays Clay Minerals,* 37, 385, 1989.
41. **Thomas, J. K.,** Photochemical and photophysical processes on clay surfaces, *Acc. Chem. Res.*, 21, 275, 1988.
42. **Pinnavaia, T. J.,** Intercalated clay catalysts, *Science* 220, 365, 1983.
43. **Nakamura, T. and Thomas, J. K.,** Formation of surfactant double layers on laponite clay colloids, *Langmuir,* 3, 234, 1987.
44. **Schoonheydt, R. A., Pauw, P. D., Vliers, D., and DeSchryver, F. C.,** Luminescence of tris(2,2-bipyridine)ruthenium(II) in aqueous clay mineral suspensions, *J. Phys. Chem.*, 88, 5113, 1984.
45. **Viaene, K., Schoonheydt, R. A., Crutzen, M., Kunyima, B., and DeSchryver, F. C.,** Study of the adsorption on clay particles by means of fluorescent probes, *Langmuir,* 4, 749, 1988.
46. **Labbec P. and Reverdy, G.,** Adsorption characteristics of polycyclic aromatic compounds on clay: pyrene as a photophysical probe on laponite, *Langmuir,* 4, 419, 1988.
47. **Chander, P., Somasundaram, P., Turro, N. J., and Waterman, K. C.,** Excimer fluorescence determination of solid-liquid interfacial poly(acrylic acid) conformations, *Langmuir,* 3, 298, 1987.
48a. **Breck, D. W.,** *Zeolite Molecular Sieves,* Wiley, New York, 1974.
48b. **Robo, J. A.,** *Zeolite Chemistry and Catalysis, ACS Monograph Series,* No. 171, American Chemistry Society Washington D.C., 1976.
48c. **Van Hooft, J. H. C.,** *Chemistry and Chemical Engineering of Catalytic Process, NATO Advanced Studies Institute Series E. No. E39,* Prins, R. and Schuit, G. C. A., Eds., Sijthoff & Noordhoff Publishers, The Netherlands, 1980, 161.
49. **Casal, H. L. and Scaiano, J. C.,** Intrazeolite photochemistry. II. Evidence for site inhomogeneity from studies of aromatic ketone phosphorescence, *Can. J. Chem.*, 63, 1308, 1985.
50a. **Casal, H. L. and Scaiano, J. C.,** Intrazeolite photochemistry. I. Phosphorescence enhancement of aromatic ketones included in silicalite, *Can. J. Chem.*, 62, 628, 1984.
50b. **Liu, X., Iu, K.-K., and Thomas, J. K.,** *J. Phys. Chem.*, 93, 4120, 1989.
51. **Abdel-kader, M. H., Hamzah, R. Y., and Abdel-Halim, S. T.,** Photochemical cis/trans isomerization of an amphiphilic merocyanine dye in homogeneous solutions and reversed micelles, *Photochem. Photobiol.*, 50, 599, 1989.
52. **Takagi, K., Fukaya, H., Miyake, N., and Sawaki, Y.,** Organized photodimerization of cinnamic acid in cationic reversed micelle, *Chem. Lett.*, p. 1053, 1988.
53. **Rachinskii, A. G. and Razumov, V. F.,** Photochemical properties of 1,2-di-1-naphthylethylene in micellar solutions, *Izv. Akad, Nauk, SSSR, Ser. Khim.*, p. 2742, 1988.

54. **Fanghaenel, E., Ortmann, W., and Hennig, A.,** 1,2,3-Triazabutadienes, XX. Investigation of the photochemical Z-E isomerization, photolysis, protonation and acidic cleavage of 1-aryl-3-(3-methyl-2-benzothiazovinylidene)triazenes in micellar solutions, *J. Prakt. Chem.*, 330, 27, 1988.

55. **Gessner, F., Olea, A., Lobaugh, J. H., Johnston, L. J., and Scaiano, J. C.,** Intrazeolite photochemistry. V. Use of zeolites in the control of photostationary ratios in sensitized cis-trans isomerization, *J. Org. Chem.*, 54, 259, 1989.

56a. **Takagi, K., Usami, H., Fukaya, H., and Sawaki, Y.,** Sapatially controlled photocycloaddition of a clay-intercalated stilbazolium cation, *J. Chem. Soc. Chem. Commun.*, p. 1174, 1989.

56b. **Usami, H., Takagi, K., and Sawaki, Y.,** Controlled photocycloaddition of stilbazolium ions intercalated in saponite clay layers, *J. Chem. Soc. Perkin Trans.*, 2, 1723, 1990.

56c. **Usami, H., Takagi, K., and Sawaki, Y.,** Effect of alkylammonium ions on the photochemical behaviors of stilbazolium aggregates in clay interlayers, *Bull. Chem. Soc. Jpn.*, 64, 3395, 1991.

57. **Takagi, K., Shichi, T., Usami, H., and Sawaki, Y.,** Photocyclodimerization of cinnamic acids intercalated in hydrotalcite, *J. Am. Chem. Soc.*, 115, 4339, 1993.

58. **Zawadzki, M. E. and Ellis, A. B.,** Silica gel mediated photoisomerization of retinal isomers and comparisons with other forms of environmental perturbation, *J. Org. Chem.*, 48, 3156, 1983.

59. **Breuer, H. D. and Jacobs, H.,** Photoisomerization of thioindigo adsorbed on alumina, *Chem. Phys. Lett.*, 73, 172, 1980.

60a. **Worsham, P. R., Eaker, D. W., and Whitten, D. G.,** Ketone photoreactivity as a probe of the microenvironment: photochemistry of the surfactant ketone 16-oxo-16-p-tolylbevadecanoic acid in monolayers, micelles, and solution, *J. Am. Chem. Soc.*, 100, 7091, 1978.

60b. **Winkle, J. R., Worsham, P. R., Shanze, K. S., and Whitten, D. G.,** Photoreactivity of surfactant ketones as a probe of microenvironment of organized media, *J. Am. Chem. Soc.*, 105, 3951, 1983.

61. **Zachariasse, K. A.,** Intermolecular excimer formation with diarylalkanes as a microfluidity probe for sodium dodecyl sulfate micelles, *Chem. Phys. Lett.*, 57, 429, 1978.

62. **Hrovat, D. A., Lin, J. H., Turro, N. J., and Weiss, R. G.,** Type II photochemistry of ketones in ligand crystalline solvents. The influence of ordered media on biradical dynamics, *J. Am. Chem. Soc.*, 106, 7033, 1984.

63. **Turro, N. J. and Wan, P.,** Photochemistry of phenyl alkyl ketones adsorbed on zeolite molecular sieves. Observation of pronounced effect on type I/II photochemistry, *Tetrahedron Lett.*, 25, 3655, 1984.

64a. **Corbin, D., Eaton, D. F., and Ramamurthy, V.,** Modification of photochemical reactivity by zeolites: Norrish type I and type II reactions of benzoin derivatives, *J. Am. Chem. Soc.*, 110, 4848, 1988.

64b. **Ramamurthy, V., Turro, N. J., and Sato, Y.,** Modification of photochemical reactivity by zeolite: cation enhanced α-cleavage of aryl alkyl ketones induced in faujasites, *Tetrahedron Lett.*, 30, 5829, 1989.

64c. **Ramamurthy, V., Casper, J. V., Eaton, D. F., Kuo, E. W., and Corbin, D. R.,** Heavy-atom-induced phosphorescence of aromatics and olefins included within zeolites, *J. Am. Chem. Soc.*, 114, 3882, 1992.

65. **Turro, N. J. and Cherry, W. R.,** Photoreactions in detergent solutions. Enhancement of regioselectivity resulting from the reduced dimentionality of substrates sequestered in a micelle, *J. Am. Chem. Soc.*, 100, 7431, 1978.

66. **Turro, N. J. and Kraeuther, B.,** Magnetic isotope and magnetic field effects on chemical reactions. Sunlight and soap for the efficient separation of ^{13}C and ^{12}C isotopes, *J. Am. Chem. Soc.*, 100, 7432, 1978.

67a. **Turro, N. J. and Kraeuther, B.,** Magnetic field and magnetic isotope effects in organic photochemical reactions. A novel probe of reaction mechanisms and a method for environment of magnetic isotopes, *Acc. Chem. Res.*, 13, 369, 1980.

67b. **Hwang, K. C., Roth, H. D., Turro, N. J., and Welsh, K. M.,** *J. Phys. Org. Chem.*, 5, 209, 1992.

68. **Turro, N. J.,** Influence of nuclear spin on chemical reactions: magnetic isotope and magnetic field effects, *Proc. Natl. Acad. Sci. U.S.A.*, 80, 609, 1983.

69. **Turro, N. J., Zimmt, J., Mathew, B., and Gould, I. R.,** Dynamics of micellized radical pairs. Measurement of micellar exit rates of benzylic radicals, *J. Am. Chem. Soc.*, 105, 6347, 1983.

70. **Ghatlia, N. and Turro, N. J.,** Diastereoselective induction in radical coupling reactions: photolysis of 2,4-diphenyl-pentan-3-ones adsorbed on faujasite zeolites, *J. Photochem. Photobiol. A: Chem.*, 57, 7, 1991.

71. **Turro, N. J., Amderson, D. R., and Kraeuther, B.,** Photochemistry of ketones in micellar solution: structural and viscosity effects on carbon-13 isotope enrichment, *Tetrahedron Lett.*, 21, 3, 1980.

72. **Beretz, B. H. and Turro, N. J.,** Photochemistry of diastereomeric 2,4-diphenyl-pentan-3-ones and related ketones in "super-cage" environments provided by micelles, porous glass, and porous silica: temperature and magnetic field effects, *J. Am. Chem. Soc.*, 105, 1309, 1983.

73a. **Kabasakalian, P. and Townley, E. R.,** Photolysis of nitrite esters in solutions. I. Photochemistry of n-octyl nitrite, *J. Am. Chem. Soc.*, 84, 2711, 1962.

73b. **Law, K.-Y. and de Mayo, P.,** Biphasic photochemistry: use of the Barton reactions to determine micelle viscosity, *J. Chem. Soc. Chem. Commun.*, p. 1110, 1978.

74a. **Ampo, M., Wada, T., and Kubokawa, Y.,** Photochemistry in the adsorbed layer. VIII. Lifetimes of excited alkyl ketones and alkyl radicals adsorbed on porous Vycor glass, *Bull. Chem. Soc. Jpn.*, 50, 31, 1977.

74b. **Hsu, W. L. and Lin, C. T.,** Chemical and physical transformations of aromatic carbonyls embedded in Vycor glass, *J. Phys. Chem.*, 94, 3780, 1990.

75a. **Turro, N. J., Chang, C.-C., Abrams, L., and Corbin, D. R.,** Size, shape, and site selectivities in the photochemical reactions of molecules adsorbed on pentasil zeolites. Effects of coadsorbed water, *J. Am. Chem. Soc.*, 109, 2449, 1978.

75b. **Dutta, P. K. and Turbeville, W.,** Examination of the solventlike nature of zeolite based on a solvatochromic indicator, *J. Phys. Chem.*, 95, 4087, 1991.

76a. **Turro, N. J.,** Photochemistry of organic molecules in microscopic reactors, *Pure Appl. Chem.*, 58, 1219, 1986.

76b. **Turro, N. J. and Zhang, Z.,** Magnetic isotope and magnetic field effects on the product distributions of photolyses of dibenzyl ketone adsorbed on zeolites, *Tetrahedron Lett.*, 30, 3761, 1989.

76c. **Ramamurthy, V., Corbin, D. R., Eaton, D. F., and Turro, N. J.,** Modification of photochemical reactivity by zeolites: role of cations in controlling the behavior of radicals generated within faujasites, *Tetrahedron Lett.*, 30, 5833, 1989.

77. **Garcia-Garibay, M., Zhang, Z., and Turro, N. J.,** Diffusion and percolation of radical pairs in zeolite media. A product analysis study, *J. Am. Chem. Soc.*, 113, 6212, 1991.

78. **Turro, N. J., Cheng, C.-C., Lei, X.-G., and Flanigen, E. M.,** Size and selectivity in zeolite chemistry. A remarkable effect of additive on the products produced in the photolysis of ketones, *J. Am. Chem. Soc.*, 107, 3739, 1985.

79. **Turro, N. J., Lei, X., Cheng, C.-C., Corbin, D. R., and Abrams, L.,** Photolysis of dibenzylketones in the presence of pentasil zeolites. Examples of size/shape selectivity and molecular diffusional traffic control, *J. Am. Chem. Soc.*, 107, 5824, 1985.

80. **Wagner, P. J. and Stratton, T. J.,** Kinetically distinct triplets in the photorearrangement of 2-phenylcyclohexanone to *cis*- and *trans*-6-phenyl-5-hexanals, *Tetrahedron*, 37, 3317, 1981.

81. **Zimmt, M. B., Doubleday, C. E., Jr., Gould, I. R., and Turro, N. J.,** Magnetic field effect on the intersystem crossing rate constants of biradicals measured by nanosecond transient UV absorption, *J. Am. Chem. Soc.*, 107, 6726, 1985.

82. **Lei, X., Doubleday, C. E., Jr., Zimmt, M. B., and Turro, N. J.,** Photochemistry of large ring 2-phenylcyclononones. Formation of cyclophanes and encapsulation by a ship in bottle and by a reptation strategy, *J. Am. Chem. Soc.*, 108, 2444, 1986.

83. **Avnir, D., deMayo, P., and Ono, I.,** Biphasic photochemistry: the photo-fries rearrangement on silica gel, *J. Chem. Soc. Chem. Commun.*, p. 1109, 1978.

84. **Magdy, M., Abdel-Malik, M. M., and deMayo, P.,** Surface photochemistry: the amide photo-fries rearrangement, *Can. J. Chem.*, 62, 1275, 1984.

85. **Wolff, T., Mueller, N., and Von Buenau, G.,** Regioselective photodimerization of 9-methylanthracene in homogeneous and micellar solutions, *J. Photochem.*, 22, 61, 1983.

86. **Wolff, T.,** Micelle-directed regioselective photodimerization of 9-hydroxymethyl anthracene, *J. Photochem.*, 16, 343, 1981.

87. **Berenjian, N., deMayo, P., Sturgeon, M.-E., Sydnes, L. K., and Weedon, A. C.,** Biphasic photochemistry: micelle solutions as media for photochemical cycloaddition of enones, *Can. J. Chem.*, 60, 425, 1982.

88. **Mayer, H., Schuster, F., and Sauer, J.,** Photochemisch induzierte (2+2)-Cycloadditionen in micellen: ein vergleich des produktspektrums mit reaktionen in losung, *Tetrahedron Lett.*, p. 1289, 1986.

89. **Quina, F. H., Möbius, D., Carroll, F. A., Hopf, F. R., and Whitten, D. G.,** Photochemical reactions in organized monolayer assemblies. II. Excimer formation and reaction in the solid state in organized monolayer assemblies, *Z. Phys. Chem. N. F.*, 101, 151, 1976.

90. **Quina, F. H. and Whitten, D. G.,** Photochemical reaction in organized monolayer assemblies. IV. Photodimerization, photoisomerization, and excimer formation with surfactant olefins and dienes in monolayer assemblies, crystals, and micelles, *J. Am. Chem. Soc.*, 99, 877, 1977.

91. **Takagi, K., Suddaby, B. R., Vadas, S. L., Backer, C. A., and Whitten, D. G.,** Topological control of reactivity by interfacial orientation: excimer fluorescence and photodimerization of 4-stilbazolium cations in aerozol OT reversed micelles, *J. Am. Chem. Soc.*, 108, 7865, 1986.

92. **Takagi, K., Nambara, E., Usami, H., Itoh, M., and Sawaki, Y.,** Organized photocyclodimerization of laurylammonium indene-2-carboxylate aggregates, *J. Chem. Soc. Perkin Trans.*, I, 655, 1991.

93a. **Lee, K. H. and deMayo, P.,** Biphasic photochemistry: photochemical regiospecificity and critical micelle concentration determination, *Photochem. Photobiol.*, 31, 311, 1980.

93b. **Lee, K. H. and deMayo, P.,** Biphasic photochemistry: micellar regioselectivity in enone dimerization, *J. Chem. Soc. Chem. Commun.*, p. 493, 1979.

94. **Fagues, R., Maurette, M. T., Oliveros, E., Riviere, M., and Lattes, A.,** Chemical and photochemical reactivity in micellar media and microemulsions. IV. Concentration effects on isophorone dimerization, *J. Photochem.*, 18, 101, 1982.

95. **Muthuramu, K. and Ramamurthy, V.,** Photodimerization of coumarin in aqueous and micellar media, *J. Org. Chem.*, 47, 3976, 1982.

96. **Ramesh, V. and Ramamurthy, V.,** Control of regiochemistry in photodimerization through micellar preorientational effect: 2-substituted naphthalenes, *J. Org. Chem.*, 49, 536, 1984.
97. **Nakamura, Y., Kato, T., and Morita, Y.,** A micellar alignment effect in the photodimerizations of N-ϖ-carboxyalkyl-2-pyridones and their 4-alkyl derivatives in micelle or reversed micelle, *Tetrahedron Lett.*, 22, 1025, 1981.
98. **Bauer, R. K., Borenetein, Jr., deMayo, P., Okada, K., Rafalska, M., Ware, W. R., and Wu, K. C.,** Surface photochemistry: translational motion of organic molecules adsorbed on silica gel and its consequences, *J. Am. Chem. Soc.*, 104, 4635, 1982.
99. **Kessler, R. W. and Wilkinson, L.,** Diffuse reflectance triplet-triplet absorption spectroscopy of aromatic hydrocarbones chemisorbed on γ-alumina, *J. Chem. Soc. Faraday Trans.*, 77, 309, 1981.
100a. **Turro, N. J., Zimmt, M. B., Gould, I. R., and Mahler, W.,** Triplet energy transfer as a probe of surface diffusion rates: a time-resolved diffuse reflectance transient absorption spectroscopy study, *J. Am. Chem. Soc.*, 107, 5826, 1985.
100b. **Kelly, G., Willsher, C. J., Wilkinson, F., Netto-Ferreira, J. C., Olea, A., Weir, D., Johnston, L. J., and J. C. Scaiano,** Intrazeolite photochemistry. VI Diffuse reflectance laser flash photolysis and product studies of diphenylmethyl radicals on solid supports, *Can. J. Chem.*, 68, 812, 1990.
101. **Lagaly, G.,** Kink-block and gauche-block structures of bimolecular films, *Angew. Chem. Int. Ed. Engl.*, 15, 575, 1976.
102. **Usami, H., Takagi, K., and Sawaki, Y.,** Effect of alkylammonium ions on the photochemical behaviors of stilbazolium aggregates in clay interlayers, *Bull. Chem. Soc. Jpn.*, 64, 3395, 1991.
103. **Ramamurthy, V., Corbin, D. R., Kumar, C. V., and Turro, N. J.,** Modification of photochemical reactivity by zeolites: cation controlled photodimerization of acenaphthylene within faujasites, *Tetrahedron Lett.*, 31, 47, 1990.
104a. **deMayo, P. and Sydnes, L. K.,** Biphasic photochemistry: micellar control of regioselectivity in enone photoannelations, *J. Chem. Soc. Chem. Commun.*, p. 994, 1980.
104b. **Berenjian, N., deMayo, P., Sturgeon, M.-E., Sydnes, L. K., and Weedon, A. C.,** Biphasic photochemistry: micelle solutions as a media for photochemical cycloaddition of enones, *Can. J. Chem.*, 60, 425, 1982.
105. **Farware, R., deMayo, P., Schanble, J. H., and Toong, Y. C.,** Surface photochemistry: enone photocycloaddition by adsorbed molecules on silica gel and alumina, *J. Org. Chem.*, 50, 245, 1985.
106. **Dave, V., Farwara, R., deMayo, P., and Stothers, J. B.,** Surface photochemistry: silica gel as a medium for photochemical cycloaddition of enones to allene, *Can. J. Chem.*, 63, 2401, 1985.
107. **Breslow, R., Kitabatake, S., and Rothbard, J.,** Photoreactions of charged benzophenone with amphiphiles in micelles and multicomponent aggregates as conformational probes, *J. Am. Chem. Soc.*, 100, 8156, 1978.
108. **Mitani, M., Suzuki, T., Takeuchi, H., and Koyama, K.,** Regioselective functionalization of unactivated methylene groups induced by photochemistry in micellar solutions, *Tetrahedron Lett.*, p. 803, 1979.
109a. **Horner, L. and Klaus, J.,** Photochemisch induzierte reaktionen mit grenzflachen-gebundenen sensibilisatoren, *Liebigs Ann. Chem.*, p. 792, 1981.
109b. **Avnir, D., Wellner, E., and Ottolenghi, M.,** Photophysical recognition of chiral surfaces, *J. Am. Chem. Soc.*, 111, 2001, 1989.
110. **Hautara, R. R. and Letzinger, R. L.,** Effects of micelles on the efficiency of photoinduced substitution reactions and fluorescence quenching, *J. Org. Chem.*, 36, 3762, 1971.
111. **Yamada, K., Shigehiro, K., Kiyozuka, T., and Iida, H.,** A photoreaction of 4-nitrophenylnitromethane in micellar system, *Bull. Chem. Soc. Jpn.*, 51, 2447, 1978.
112. **Bonilha, J. B. S., Chaimovich, H., Toscano, V. G., and Quina, F. H.,** Photophenomena in surfactant media. II. Analysis of the alkaline photohydrolysis of 3,5-dinitroanisole in aqueous micellar solutions of N-tetradecyl-N,N,N-trimethylammonium chloride, *J. Phys. Chem.*, 83, 2463, 1979.
113. **Chawla, H. M. and Sharma, S. K.,** Regioselective synthesis of 2-arylidenecoumarin-3-ones by dye-sensitized photooxygenation of 2-hydroxyphenylstyrylketones in the presence of sodium dodecylsulfate, *Tetrahedron*, 46, 1611, 1990.
114a. **DeVoe, R. J., Sahyun, M. R. V., Schmidt, E., and Sharma, D. K.,** Photoxidation of 9,10-diethoxyanthracene. Mechanistic dichotomies between homogeneous solution and reversed micelle photoprocesses, *Can. J. Chem.*, 68, 612, 1990.
114b. **DeVoe, R. J., Sahyun, M. R. V., Schmidt, E., Serpone, N., and Sharma, D. K.,** Electron transfer sensitized photolysis of onium salts, *Can. J. Chem.*, 66, 319, 1988.
114c. **DeVoe, R. J., Sahyun, M. R. V., Serpone, N., and Sharma, D. K.,** Transient intermediates in the photolysis of iodonium cations, *Can. J. Chem.*, 65, 2342, 1987.
115a. **Singhal, G. S., Rabinowitch, E., Hevesi, J., and Srinivasan, V.,** Migration of excitation energy from thionine to methylene blue in micelles, *Photochem. Photobiol.*, 11, 537, 1970.
115b. **Kenney-Wallace, G. A., Flint, J. H., and Wallace, S. C.,** Resonance energy transfer between lasing dyes in micellar media, *Chem. Phys. Lett.*, 32, 71, 1975.
115c. **Matsuo, T., Aso, Y., and Kano, K.,** Energy transfer in micellar systems, fluorescence investigation of energy transfer from dialkylalloxazine to dye cations

in the presence of anionic micelles, *J. Phys. Chem.*, 84, 146, 1980.

115d. **Koglin, P. K. F., Miller, D. J., Steinwandel, J., and Hauser, M.,** Determination of micelle aggregation numbers by energy transfer, *J. Phys. Chem.*, 85, 2363, 1981.

116a. **Möbius, D.,** Designed monolayer assemblies, *Ber. Bunsenges. Phys. Chem.*, 82, 848, 1978.

116b. **Seefeld, K.-P., Möbius, D., and Kuhn, H.,** Electron transfer in monolayer assemblies with incorporated ruthenium(II) complexes, *Helv. Chim. Acta*, 60, 2608, 1977.

117. **Inacker, O. and Kuhn, H.,** Discrimination between different paths of deactivation of excited dye molecules by monolayer techniques, *Chem. Phys. Lett.*, 28, 15, 1974.

118a. **Kavarnos, G. J. and Turro, N. J.,** Photosensitization by reversible electron transfer: theories, experimental evidence, and examples, *Chem. Rev.*, 86, 401, 1986.

118b. **Fox, M., Ed.,** *Photoinduced Electron Transfers, Parts B and D*, Elsevier, Amsterdam, 1988.

119. **Takagi, K. and Sawaki, Y.,** Photosensitized electron transfer reactions utilizing ionic interface, *Hyomen(Surface)*, 28, 161, 1990.

120. **Kano, K., Takuma, K., Ikeda, T., Nakajima, D., Tsutsui, Y., and Matsuo, T.,** Zinc tetraphenylporphyrin-sensitized photoreduction of anthraquinonesulfonate in aqueous micellar solutions, *Photochem. Photobiol.*, 27, 695, 1978.

121. **Tsutsui, Y., Takuma, K., Nishijima, T., and Matsuo, T.,** Photoreduction and redox catalysis of an amphipathic derivative of *tris*(2,2′-bipyridine) ruthenium (II) at the micellar surface, *Chem. Lett.*, p. 617, 1979.

122. **Takayanagi, T., Nagamura, T., and Matsuo, T.,** Photoinduced electron transfer between amphipathic ruthenium(II) complex and N-butylphenotiazine in various microenvironments, *Ber. Bunsenges. Phys. Chem.*, 84, 1125, 1980.

123. **Nagamura, T., Takuma, K., Tsutsui, Y., and Matsuo, T.,** Photoinduced electron transfer between amphipathic ruthenium(II) complex and N,N-dimethylaniline in synthetic bilayer membranes and phospholipid liposomes, *Chem. Lett.*, p. 503, 1980.

124. **Inoue, H. and Hida, M.,** Photochemical electron transfer from water layer to organic layer via sodium anthraquinone-2-sulfonate by stepwise two photon excitation, *Bull. Chem. Soc. Jpn.*, 55, 1880, 1982.

125. **Degani, Y. and Willner, I.,** Complex formation between anthraquinone-2,6-disulfonate and a neutral zin porphyrin. Effects of CTAB micelles on complex stability and photoinduced electron transfer, *J. Phys. Chem.*, 89, 5685, 1985.

126. **LeMoigne, J., Gramain, P., and Simon, J.,** Fast cation transfer at a micelle subsurface: synthesis and properties of an amphiphilic macrocycle, *J. Phys. Chem.*, 60, 565, 1977.

127. **Humphry-Baker, R., Grätzel, M., Tundo, P., and Pelizzeti, E.,** Complexes of nitrogen containing crown ether surfactants with stable silver atoms, *Angew. Chem. Int. Ed., Engl.*, 18, 630, 1979.

128. **Humphry-Baker, R., Moroi, Y., Grätzel, M., Pelizzetti, E., and Tundo, P.,** Photoinduced processes in copper(ii)-crown ether surfactant micelles, *J. Am. Chem. Soc.*, 102, 3689, 1980.

129. **Moroi, Y., Braun, A. M., and Grätzel, M.,** Light-initiated electron transfer in functional surfactant assemblies. I. Micelles with transition metal counterions *J. Am. Chem. Soc.*, 101, 567, 1979.

130. **Jones, G., II and Goswami, K.,** The photochemistry of triarylmethane dyes bound to polyelectrolytes: photoinduced electron transfer involving bound dye monomers and dimers, *J. Photochem. Phobiol. A: Chem.*, 57, 65, 1991.

131a. **Degani, Y. and Willner, I.,** Photoinduced hydrogen evolution of a zwitterionic diquat electron acceptor. The functions of SiO_2 colloid in controlling the electron transfer process, *J. Am. Chem. Soc.*, 105, 6228, 1983. Electron-transfer reactions of quinons, hydroquinones, and methyl viologen sensitized by *tris*(2,2-bipyridine)-ruthenium (II), *J. Chem. Soc. Faraday Trans. 2.*, 77, 373, 1980.

131b. **Birenbaum, H., Avhir, D., and Ottolenghi, M.,** Surface geometry and pore-size effects on photoinduced charge-transfer interactions between pyrene and diethylaniline on silica surfaces, *Langmuir*, 5, 48, 1989.

132. **Moroi, Y., Infelta, P. P., and Grätzel, M.,** Light-initiated redox reactions in functional assemblies. II. Dynamics in europium (III) surfactant solutions, *J. Am. Chem. Soc.*, 101, 573, 1979.

133. **Tabushi, I., Yazaki, A., Koga, N., and Iwasaki, K.,** Artificial photosynthesis system of bacteria type, *Tetrahedron Lett.*, 21, 373, 1980.

134. **Tabushi, I. and Kugimiya, S.,** Phase-transfer-aided FMNH production using artificial photosynthesis cells of bacterial type cell system optimization by the concept of flux conjugation, *J. Am. Chem. Soc.*, 107, 1859, 1985.

135. **Maidan, R., Goren, Z., Becker, J. Y., and Willner, I.,** Application of multielectron charge relays in chemical and photochemical debromination processes. The role of induced disproportionation of N,N′-dioctyl-4,4′-bipyridinium radical cation in two-phase systems, *J. Am. Chem. Soc.*, 106, 6217, 1984.

136. **Khannanov, N. K., Kuz'min, V. A., Levin, P. P. Slatirovish, V. Y., and Yablonskaya, E. E.,** Efficiency of spatial charge separation in the vesicular system: *tris*(2,2′-bipyridine)ruthenium(II) (internal solution)-octadecylviologen(membrane)-oxidant (external solution), *Khim. Fiz.*, 5, 1359, 1986.

137. **Yablonskaya, E. E., Nadtochenko, V. A., and Shafirovich, V. Y.,** Reduction of membrane-bound viologen photosensitized by zinc meso-tetra(4-N-methyl-pyridyl)porphyrin encapsulated into lipid vesicle

inner volume, *Izv. Akad. Nauk. SSSR, Ser. Khim.*, p. 334, 1986 (*Chem. Abstr.*, 106, 2294c, 1987).

138. **Shafirovich, V. Y., Levin, P. D., Khannanov, N. K., and Kuz'min, V. A.,** Electron transfer through a bilayer lipid membrane-aqueous solution interface and the kinetics of oxidation of viologen radicals in homogeneous and vesicular system, *Izv. Akad. Nauk SSSR, Ser. Khim.*, p. 801, 1986 (*Chem. Abstr.*, 105, 114485d, 1986).
139. **Calvin, M.,** Simulating photosynthetic quantum conversion, *Acc. Chem. Res.*, 11, 369, 1978.
140. **Ferd, W. E., Otvos, J. W., and Calvin, M.,** Photosensitized electron transfer across phospholipid vesicle walls, *Nature*, 274, 507, 1978.
141. **Matsuo, T., Itoh, K., Takuma, K., Hashimoto, K., and Nagamura, T.,** A concerted two-step activation of photoinduced electron-transport across lipid membrane, *Chem. Lett.*, p. 1009, 1980.
142. **Tabushi, I., Kugimiya, S., and Mizutani, T.,** Photoreduction of keto carboxylic acid derivatives to oxyacid derivatives by ZnTPPS-quinolinium-3-carboxamide-CTAB micelle, *J. Am. Chem. Soc.*, 105, 1658, 1983.
143a. **Alkaitis, S. A. and Grätzel, M.,** Laser photoisomerization of phenothiazine in alcoholic and aqueous micellar solution. Electron transfer from triplet states to metal ion acceptors, *J. Am. Chem. Soc.*, 98, 5703, 1975.
143b. **Alkaitis, S. A., Grätzel, M., and Henglein, A.,** Laser photo-ionization of phenothiazine in micellar solution. II. mechanism and light induced redox reactions with quinones, *Ber. Bunsenges. Phys. Chem.*, 79, 541, 1975.
143c. **Alkaitis, S. A. and Grätzel, M.,** Laser photoisomerization and light-initiated redox reactions of tetramethylbenzidine in organic solvents and aqueous micellar solution, *J. Am. Chem. Soc.*, 98, 3549, 1976.
144. **Takagi, K., Miyake, N., Nakamura, E., Sawaki, Y., Koga, N., and Iwamura, H.,** ZnTPPS-sensitized photodebromination of 2,3-dibromo-3-phenylpropionic acids. Electron transfer initiated chain debromination, *J. Org. Chem.*, 53, 1703, 1988.
145. **Takagi, K., Fukaya, H., and Sawaki, Y.,** Does a stilbazolium cation adsorbing poly(styrenesulfonate) anion form micellelike clusters? *J. Am. Chem. Soc.*, 110, 7469, 1988.
146. **Takagi, K., Aoshima, K., and Sawaki, Y.,** Electron-relay chain reaction of N-methyl 4-β-styrylpyridinium ion on colloidal silica, *J. Chem. Soc. Perkin Trans.*, II, 1771, 1986.
147. **Villemure, G., Kodama, H., and Detellier, C.,** Photoreduction of water by visible light in the presence of montmorillonite, *Can. J. Chem.*, 63, 1139, 1985.
148. **Villemure, G., Detellier, C., and Szabo, A. G.,** Fluorescence of clay-intercalated methylviologen, *J. Am. Chem. Soc.*, 108, 4658, 1986.
149. **Ghosh, P. K. and Bard, A. J.,** Photochemistry of *tris*(2,2′-bipyridyl)ruthenium (II) in colloidal clay suspensions, *J. Phys. Chem.*, 88, 5519, 1984.
150. **Habti, A., Keravis, D., Levitz, P., and van Damme, H.,** Influence of surface heterogeneity on the luminescence decay of probe molecules in heterogeneous systems $Ru(bpy)_3^{2+}$ on clays, *J. Chem. Soc. Faraday Trans. 2*, 80, 67, 1984.
151. **DellaGuardia, R. A. and Thomas, J. K.,** Photoprocesses on colloidal clay systems, *tris*(2,2′-bipyridine)ruthenium (II) bound to colloidal kaoline and montmorillonite, *J. Phys. Chem.*, 87, 990, 1983.
152. **Nijs, H., van Damme, H., Bergaya, F., Habti, A., and Fripiat, J. J.,** Structural aspects in the photooxidation and photoreduction of water in clay mineral suspension, *J. Mol. Cat.*, 21, 223, 1983.
153. **Nijs, H., Fripiat, J. J., and van Damme, H.,** Visible-light-induced cleavage of water in colloidal clay suspensions: a new example of oscillatory reaction at interfaces, *J. Phys. Chem.*, 87, 1279, 1983.
154a. **Dutta, P. K. and Incavo, J. A.,** Photoelectron transfer from *tris*(2,2′-bipyridine)-ruthenium(II) to methyl viologen zeolite cages: a resonance Raman spectroscopic study, *J. Phys. Chem.*, 91, 4443, 1987.
154b. **Sankararaman, S., Yoon, K. B., Yabe, T., and Kohhi, J. K.,** Control of back electron transfer from charge-transfer ion pairs by zeolite supercages, *J. Am. Chem. Soc.*, 113, 1419, 1991.
155. **Krueger, J. S., Mayer, J. E., and Mallouk, T. E.,** Long-lived light-induced charge separation in a zeolite L-based molecular triad, *J. Am. Chem. Soc.*, 110, 8232, 1988.
156. **Willner, I., Eiden, Y., and Joselevish, E.,** Photosensitized electron-transfer reactions and H_2 evolution in organized microheterogeneous environments: separation of ground-state xenthene-bipyridinium complexes by SiO_2 colloids, *J. Phys. Chem.*, 94, 3092, 1990.
157. **Domen, K., Kudo, A., Shinozaki, A., Tanaka, A., Maruya, K., and Onishi, T.,** Decomposition of water and hydrogen evolution from aqueous methanol solution over novel niobrate photocatalysts, *J. Chem. Soc. Chem. Commun.*, p. 356, 1986.
158. **Domen, K., Kudo, A., Shibata, M., Tanaka, A., Maruya, K., and Onishi, T.,** Novel photocatalysts, ion-exchanged $K_4Nb_6O_{17}$, with a layer structure, *J. Chem. Soc. Chem. Commun.*, p. 1706, 1986.
159. **Nakato, T., Kuroda, K., and Kato, C.,** Photoreduction of methylviologen in the interlayer of $K_4Nb_6O_{17}$, *J. Chem. Soc. Chem. Commun.*, p. 1144, 1989.
160. **Yoon, K. B. and Koshi, J. K.,** Direct observations of superoxide electron transfer with viologens by immobilization in zeolite, *J. Am. Chem. Soc.*, 110, 6586, 1988.
161. **Howe, R. F. and Timmer, W. C.,** Esr studies of O_2^-· adsorbed on silica gel: photoformation and rotational dynamics, *J. Chem. Phys.*, 85, 6129, 1986.